State of Oregon
Oregon Department of Geology and Mineral Industries
Brad Avy, State Geologist

OPEN-FILE REPORT O-19-09

COSEISMIC LANDSLIDE SUSCEPTIBILITY, LIQUEFACTION SUSCEPTIBILITY, AND SOIL AMPLIFICATION CLASS MAPS, CLACKAMAS, COLUMBIA, MULTNOMAH, AND WASHINGTON COUNTIES, OREGON

FOR USE IN HAZUS: FEMA'S METHODOLOGY FOR ESTIMATING POTENTIAL LOSSES FROM DISASTERS

By Christina A. Appleby, William J. Burns, Robert W. Hairston-Porter, and John M. Bauer

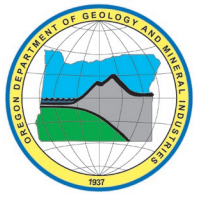

2019

Oregon Department of Geology and Mineral Industries, 800 NE Oregon Street, Suite 965, Portland, OR 97232

DISCLAIMER

This product is for informational purposes and may not have been prepared for or be suitable for legal, engineering, or surveying purposes. Users of this information should review or consult the primary data and information sources to ascertain the usability of the information. This publication cannot substitute for site-specific investigations by qualified practitioners. Site-specific data may give results that differ from the results shown in the publication.

Expires 12/31/2020

Oregon Department of Geology and Mineral Industries Open-File Report O-19-09
Published in conformance with ORS 516.030

For additional information:
Administrative Offices
800 NE Oregon Street, Suite 965
Portland, OR 97232
Telephone (971) 673-1555
https://www.oregongeology.org/
https://oregon.gov/DOGAMI/

TABLE OF CONTENTS

LIST OF FIGURES

LIST OF TABLES

GEOGRAPHIC INFORMATION SYSTEM (GIS) DATA

See the digital publication folder for files including an Esri® formatted geodatabase.
Metadata is embedded in the geodatabase and is also provided as separate .xml format files.

Coseismic_geohazard_datasets.gdb:

Feature classes:

Soil Amplification Class and Landslide Geologic Group

Liquefaction Susceptibility

Rasters:

Wet Landslide Susceptibility

Dry Landslide Susceptibility

Table:

Reference Table

1.0 REPORT SUMMARY

The Portland region, the most densely populated area in the state of Oregon, is vulnerable to both regional earthquakes from the Cascadia Subduction Zone and events on local faults like the Portland Hills fault. When an earthquake occurs, surficial geology at a given location will impact the local experience of ground motion and ground deformation. By leveraging the best available surficial geologic maps and lidar-based topographic maps, we created new coseismic geohazard maps to inform earthquake models. These models allow us to estimate the impact of an earthquake at a neighborhood-scale with greater accuracy.

The objective of this study was to produce four coseismic geohazard GIS datasets and associated maps covering Clackamas, Columbia, Multnomah, and Washington Counties, Oregon. Maps made from these datasets can be used in a Hazus-software based earthquake damage model. The maps are:

- **Two coseismic landslide susceptibility maps (wet and dry scenario):** We followed the coseismic landslide susceptibility method by Wilson and Keefer (1985) and Wieczorek and others (1985) outlined in the Hazus technical manual (FEMA, 2011). With this method, three factors determine the final landslide susceptibility class: 1) wet or dry groundwater conditions, 2) slope angle, and 3) geologic materials. We classified all areas into one of eleven landslide susceptibility classes, ranging from none to 10. The class dictates coefficients used to calculate the probability of landsliding and landslide ground deformation for a given earthquake.
- **Liquefaction susceptibility map:** We used the liquefaction susceptibility classification scheme by Youd and Perkins (1978) as used in Hazus (FEMA, 2011). The susceptibility classes are none, very low, low, moderate, high, and very high; in Hazus, they are labeled 0 to 5, respectively. Within the Hazus earthquake impact methodology, the classes are associated with coefficients used by Hazus to calculate the probability of liquefaction and the resulting permanent ground displacement for a given earthquake scenario (FEMA, 2011).
- **Soil amplification class map:** This map shows ground motion amplification changes based on physical properties of the soil column. We categorized all geologic units (including landslides) into one of six classes developed by the National Earthquake Hazard Reduction Program (NEHRP) (FEMA, 2003). The six NEHRP classes are hard rock (type A), rock (type B), very dense soil and soft rock (type C), stiff soils (type D), soft soils (type E), and soils requiring site-specific evaluations (type F). NEHRP classes are defined by the average speed at which a shear-wave propagates through the upper 30 meters (98 feet) of ground.

The data can be used to help communities become more resilient to future earthquakes and coseismic hazards. The methods and results of this study are intended for Hazus-specific mapping and are not to be used in place of site-specific mapping. For example, the data produced by this study were used to estimate the impact of potential earthquakes on current buildings and infrastructure and to estimate casualties and long-term displaced population as described in DOGAMI Open-File Report O-18-02, *Earthquake regional impact analysis for Clackamas, Multnomah, and Washington Counties, Oregon* (Bauer and others, 2018).

This work was funded by the Regional Disaster Preparedness Organization (RDPO), an organization that aims to increase the region's resiliency to disasters in the Portland metropolitan region.

2.0 INTRODUCTION

Clackamas, Columbia, Multnomah, and Washington Counties include some of the most densely populated areas in the state of Oregon and together contain nearly half of Oregon's total population (U.S. Census Bureau, 2019). The region is vulnerable to earthquakes from several different sources, including the Cascadia Subduction Zone and the Portland Hills crustal fault. When the next earthquake occurs, it will likely induce secondary hazards, known as coseismic hazards, including shaking amplification of the ground motions as they travel through surficial deposits, liquefaction of saturated, low cohesion deposits, and triggered landslides.

The Regional Disaster Preparedness Organization (RDPO), a partnership of local and regional government agencies, non-governmental organizations, and private-sector stakeholders representing the Portland metropolitan region, aims to increase the region's resiliency to disasters, including earthquakes. RDPO contracted with the Oregon Department of Geology and Mineral Industries (DOGAMI) to develop updated damage and loss estimates from major earthquakes for a five-county area (Clackamas, Columbia, Multnomah, and Washington Counties, Oregon, and Clark County, Washington) (Bauer and others, 2018; J. Bauer, written commun., 2019). DOGAMI used the Federal Emergency Management Agency (FEMA) software package Hazus to estimate damage and losses. Hazus provides default input data for analysis that can be replaced by more accurate regional data. To better estimate regional damage and losses, DOGAMI created coseismic soil amplification class, liquefaction susceptibility, and landslide susceptibility maps for use in Hazus analysis. This publication describes how the coseismic hazard maps were created and provides data for others to use. The study area and data reported here are confined to the four Oregon counties.

2.1 Study area

The study area is defined by the Clackamas, Columbia, Multnomah, and Washington County, Oregon, boundaries (**Figure 1**). The study area includes many of Oregon's major cities including Portland, Gresham, Beaverton, Hillsboro, and Tigard. The Columbia River bounds the study area to the north. The Willamette River flows north and bisects the study area. Other major rivers that flow through the study area include the Clatskanie, Clackamas, Nehalem, Sandy, and the Tualatin Rivers (**Figure 1**). The presence of rivers is noteworthy for this study because river valley bottoms are commonly composed of recently deposited alluvium and have high groundwater tables. These factors can have significant effects on soil amplification and liquefaction.

The topography is a mix of relatively flat valleys surrounded by higher-relief features. In the central section of the study area, these features include the Tualatin Mountains (also known as the Portland Hills), locally steep slope-banks along the rivers, and the Boring volcanoes (such as Rocky Butte, Powell Butte, and Kelly Butte, Mount Tabor, and Mount Scott). Also partially included in the study area are the Columbia River Gorge and Cascade Range to the east and the Coast Range to the west (**Figure 1**). Areas with steeper slopes are more prone to coseismic landslides.

Figure 1. Map of the study area: Columbia, Washington, Multnomah, and Clackamas Counties, Oregon.

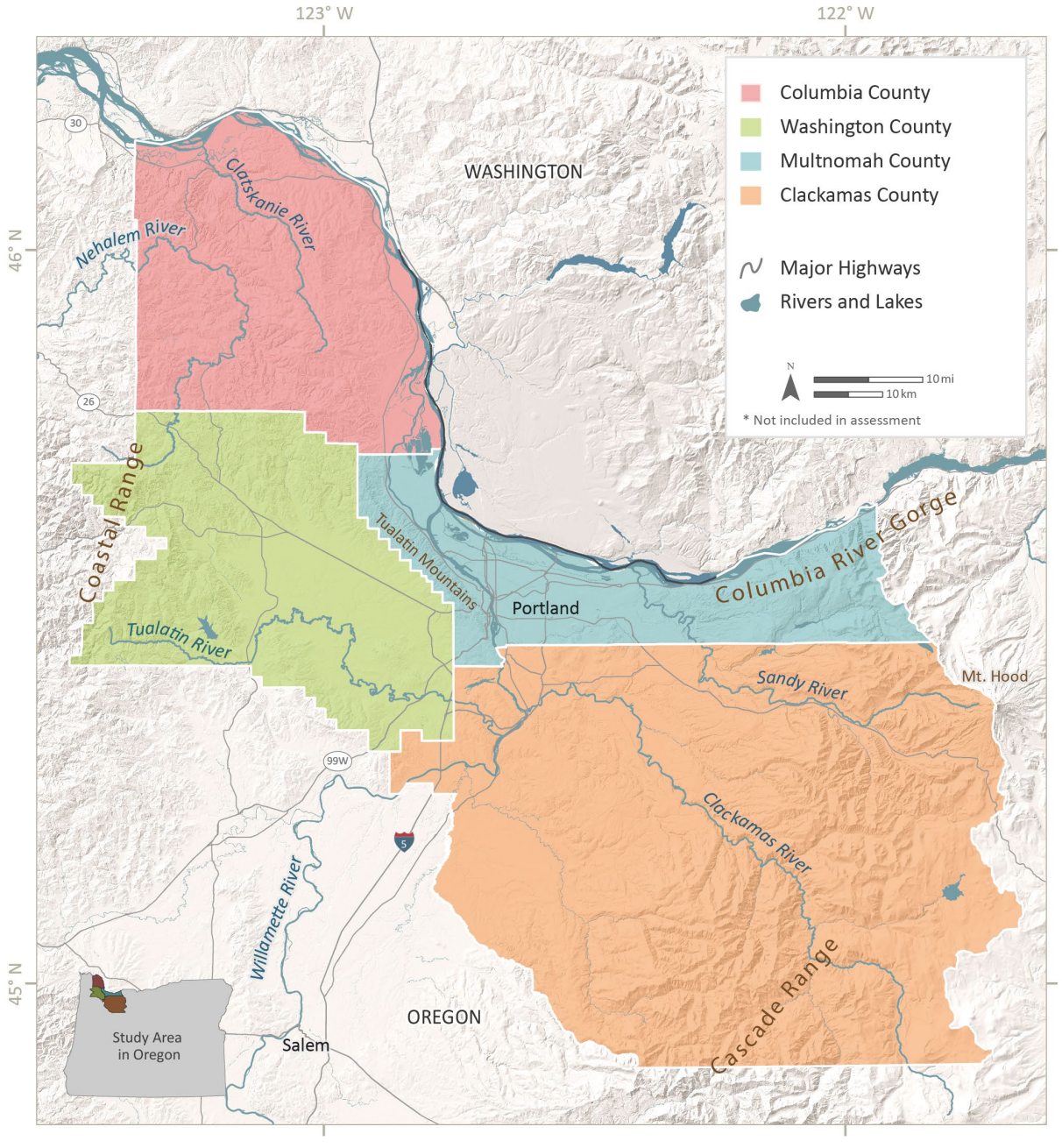

2.2 Purpose

The purpose of this project was to help communities in this region become more resilient to earthquake-induced natural hazards (coseismic hazards) by providing the communities with new maps for regional earthquake risk analysis using FEMA Hazus software (Bauer and others, 2018; J. Bauer, written commun., 2019). Hazus is a standardized methodology that contains models for estimating potential losses from earthquakes, among other hazards. The main objectives of this study included:

- Compiling the best available existing data, including previous geologic hazard reports and geologic reports
- Adjusting surficial geologic unit contacts, where needed, to align with features identified using lidar-derived topographic imagery
- Creating new or updated GIS datasets of soil amplification class, liquefaction susceptibility, and landslide susceptibility following the methods outlined in the Hazus technical manual (FEMA, 2011) and formatted for use in Hazus

The body of this report describes the methods and results for these objectives. Because the datasets were created for a specific purpose (Hazus compatibility), we caution users that the data may not be suitable for other types of analysis.

2.3 Coseismic Hazards

The most severe damage from earthquakes is often associated with the following phenomena: amplification of ground shaking by soil, ground deformation due to liquefaction of water-saturated sand, silt, or gravel, and ground deformation due to earthquake-induced landslides. Fortunately, the likelihood and severity of each of these effects can be evaluated on the basis of local geological conditions before an earthquake occurs. This study provides maps of each of these earthquake-induced hazards for each of the four counties (**Figure 1)**.

2.3.1 Soil Amplification

When an earthquake occurs, seismic waves radiate away from the hypocenter or rupture zone. In general, the strength and duration of the shaking at a site is dependent on the size of the earthquake, the distance from the hypocenter or rupture zone, and the site-specific soil characteristics (Kramer, 1996). As seismic waves travel upward to the ground surface, they encounter different types of rocks and soils that can either attenuate (weaken) or amplify (strengthen) the shaking depending on the characteristics of the rock or soil. Seismic waves travel more slowly in softer rocks and soils than in hard, solid rocks. Because soil deposits can change significantly over short distances, levels of ground-shaking amplification can also change markedly over a short distance, even if sites are at an equal distance from the earthquake source (**Figure 2**; Kramer, 1996).

Although site-specific earthquake response is complicated and depends on factors such as frequency and duration of the shaking, subsurface stratigraphy and material properties, and surface topography, useful generalizations can be made about the performance of various soils. For example, thick deposits of soft soil tend to amplify the shaking; in contrast, sites with thin soil profiles are not likely to amplify ground motions.

Figure 2. Schematic diagram of soil amplification effects on bedrock versus soft soils. (Image by M. G. Ciaccio and G. Cultrera, as cited by Rijsingen [2017]).

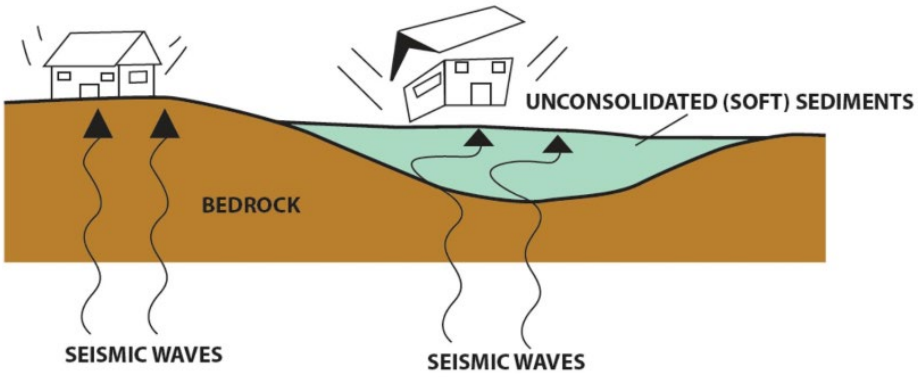

The magnitude 8.0 Mexico City earthquake in 1985 (**Figure 3**; Stone and others, 1987) provides a good example of soil amplification. During the 1985 earthquake, Mexico City, located 250 miles east of the epicenter, experienced a "highly selective" damage pattern in which the taller buildings built on soft clay and silt lake deposits experienced extensive damage while other areas sustained relatively little damage (Stone and others, 1987). Similar damage occurred in the magnitude 7.1 Puebla-Mexico City earthquake in 2017 (Geotechnical Extreme Events Reconnaissance Association [GEER], 2017).

Figure 3. Damage to a 21-story, steel-constructed apartment complex in Mexico City after the September 19, 1985, earthquake partially influenced by locally amplified ground motion. Many other factors can affect whether a building is damaged in an earthquake (Photograph from USGS https://library.usgs.gov/photo/#/item/51dc315ee4b0f81004b79efe.)

2.3.2 Liquefaction

During seismic shaking, deposits of loose, saturated non-cohesive soil can contract, resulting in an increase in pore water pressure. If the increase in pore water pressure is high enough, the deposit becomes "liquefied," losing its strength and thus its ability to support loads (Kramer, 1996).

If an earthquake induces liquefaction, several things can happen: 1) the liquefied layer and everything on top of it may move down slope, even on very gentle slopes (lateral spread), 2) the liquefied layer may oscillate with displacements large enough to rupture pipelines, move bridge abutments, or rupture building foundations, and 3) buoyant buried objects such as underground storage tanks can float toward the surface, and heavy objects such as buildings can sink. Typical lateral displacements can range from inches to yards. Liquefaction can therefore significantly increase the damage resulting from an earthquake.

An example of liquefaction can be seen by the extensive damage to infrastructure and buildings in the magnitude 6.2 February 2011 Christchurch Earthquake (**Figure 4**; GEER, 2011).

Figure 4. Examples of liquefaction damage from the February 2011 Christchurch earthquake (GEER, 2011).

2.3.3 Landslides

Strong ground shaking can also cause new landslides and reactivate dormant landslides. Commonly, slopes that are marginally stable prior to an earthquake can become unstable and fail. Some landslides result from liquefaction that causes lateral movement of soil, or lateral spread (**Figure 5**).

Figure 5. Road prism rotational type landslide (top) and lateral spread landslide along the shoreline of Capitol Lake Olympia, Washington (bottom), caused by the 2001 magnitude 6.8 Nisqually earthquake (photographs from Nisqually Earthquake Information Clearinghouse, 2001, as reproduced in Burns and others [2008] report).

2.4 Coseismic Hazard Studies in the Portland Regional Area

A number of previous regional geologic hazard studies have been conducted throughout the study area to identify and assess coseismic hazards including:

- Earthquake-hazard geology maps of the Portland metropolitan area, Oregon (Madin, 1990)
- Relative earthquake hazard map of the Portland, Oregon 7 1/2-minute quadrangle (Mabey and others, 1993a)

- Earthquake hazard maps of the Portland quadrangle, Multnomah and Washington Counties, Oregon, and Clark County, Washington (Mabey and others, 1993b)
- Relative earthquake hazard map of the Mount Tabor quadrangle, Multnomah County, Oregon, and Clark County, Washington (Mabey and others, 1995d)
- Relative earthquake hazard map of the Beaverton quadrangle, Washington County, Oregon (Mabey and others, 1995a)
- Relative earthquake hazard map of the Lake Oswego quadrangle, Clackamas, Multnomah, and Washington Counties, Oregon (Mabey and others, 1995b)
- Relative earthquake hazard map of the Gladstone quadrangle, Clackamas and Multnomah Counties, Oregon (Mabey and others, 1995c)
- Relative earthquake hazard map of the Linnton quadrangle, Multnomah and Washington Counties, Oregon (Mabey and others, 1996)
- Relative earthquake hazard map of the Portland Metro Region, Clackamas, Multnomah, and Washington Counties, Oregon (Mabey and others, 1997)
- Uniform Building Code (UBC) soil map for Oregon (Wang and others, 1998)
- Relative earthquake hazard maps for selected urban areas in western Oregon: Dallas, Hood River, McMinnville-Dayton-Lafayette, Monmouth-Independence, Newburg-Dundee, Sandy, Sheridan-Willamina, St. Helens-Columbia City-Scappoose (Madin and Wang, 1999a)
- Relative earthquake hazard maps for selected urban areas in western Oregon: Canby-Barlow-Aurora, Lebanon, Silverton-Mount Angel, Stayton-Sublimity-Aumsville, Sweet Home, Woodburn-Hubbard (Madin and Wang, 1999b)
- Relative earthquake and landslide hazards in Clackamas County (Hofmeister and others, 2003a,b)
- Multi-hazard and risk study for the Mount Hood region, Multnomah, Clackamas, and Hood River Counties, Oregon (Burns and others, 2011)
- Ground motion, ground deformation, tsunami inundation, coseismic subsidence, and damage potential maps for the 2012 Oregon Resilience Plan for Cascadia Subduction Zone Earthquakes (Madin and Burns, 2013)
- Landslide hazard and risk study of northwestern Clackamas County, Oregon (Burns and others, 2013)
- 3D geology and shear-wave velocity models of the Portland, Oregon, metropolitan area (Roe and Madin, 2013)

For the current effort, we reviewed and consolidated this large body of work to help assess hazards affecting the study area. These past studies had different purposes and methods and therefore are not necessarily comparable to this new work; however, portions of some of these past studies are foundational for this study. For example, past studies that included 3D data were reviewed and used to inform the classification process used in this study. This study improved on past works by using lidar-derived geologic data that were not available when most previous studies were conducted. Specific uses of lidar data are discussed in the following section.

3.0 METHODS

3.1 Methodology Overview

We created a set of four Hazus-compatible seismic hazard factor maps. These four maps are listed below. **Figure 6** is a flowchart summarizing the steps needed to create the maps (green boxes in the flowchart). The steps are described in detail later in this Methods section. See **Appendix B** for geologic unit classifications.

- **Unified geologic map:** First, we created two geologic maps by compiling the best available surficial geology: one with landslide features and one without landslide features (shown in **Figure 6** in grey boxes and ovals). We call these "unified" geologic maps. Both of these maps are intermediary datasets. Using features visible in the lidar-derived topography, we refined locations of geologic unit boundaries of older, non-lidar-based maps as deemed necessary.
- **Landslide susceptibility maps:** Second, we created two landslide susceptibility maps, one for wet and one for dry groundwater conditions (shown in **Figure 6** in blue boxes and ovals). These maps were derived from the unified geologic map with landslides, a list of landslide susceptibility classifications by geologic unit, and lidar-derived ground slope data.
- **Soil amplification class map:** Third, we created a soil amplification class map derived from the unified geologic map with landslides and a list of geologic unit classifications (shown in **Figure 6** in yellow boxes and ovals).
- **Liquefaction susceptibility map:** Fourth, we produced a liquefaction susceptibility map derived from the unified geologic map that did *not* include landslides and a list of geologic unit classifications (shown in **Figure 6** in orange boxes and ovals).

Figure 6. Flowchart summarizing methodology used to create soil amplification class, liquefaction susceptibility, and landslide susceptibility maps.

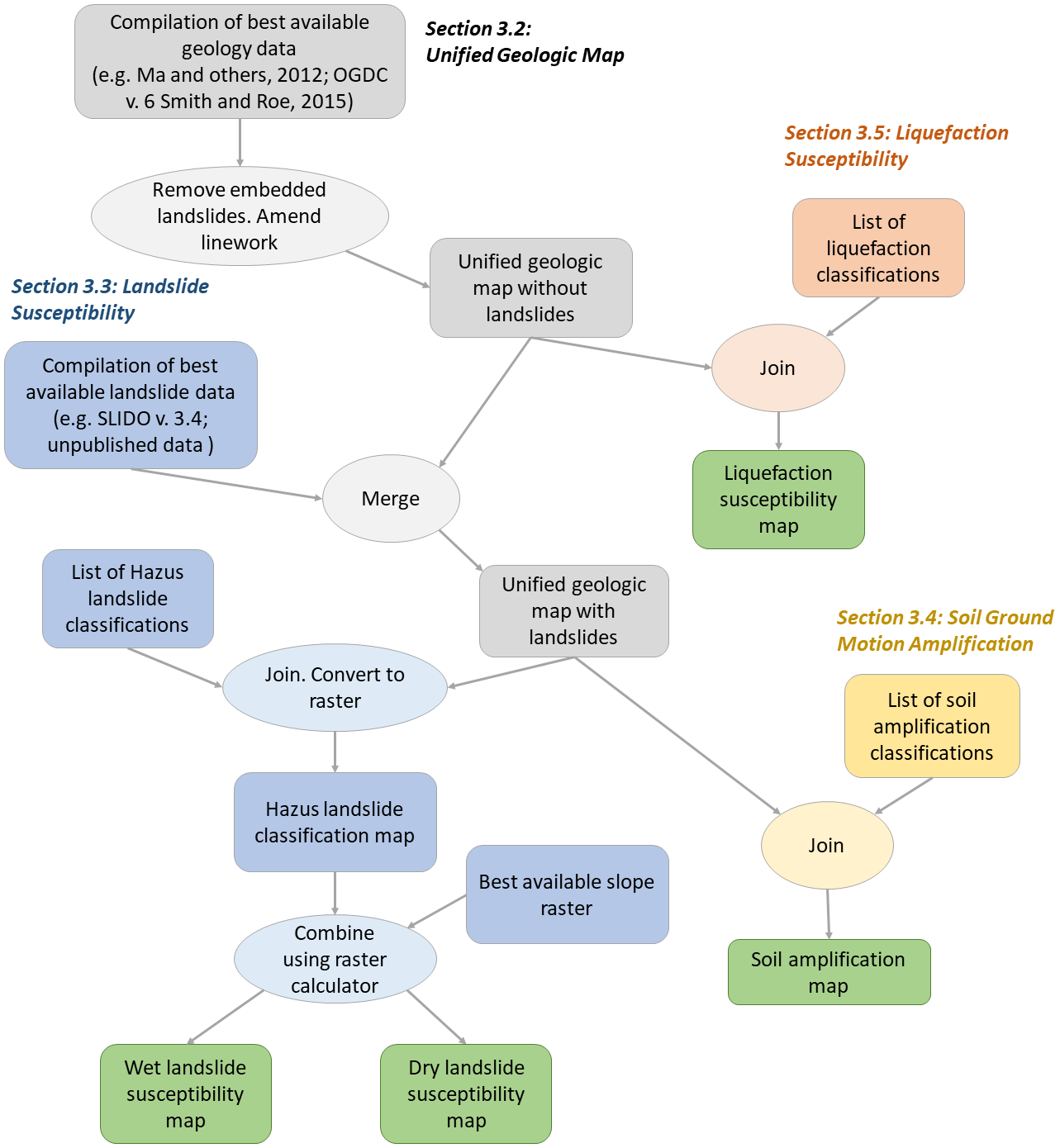

3.2 Unified Geologic Map

To produce the coseismic hazard maps, we first needed to create two versions of a unified geologic map across the study area: one geologic map with landslides and one geologic map without landslides. For both maps, we started by combining digital geologic data from the best available sources using geographic information systems (GIS) software. For this study, these sources principally included Ma and others (2012), R. Wells and others (unpub. data, 2017), Mickelson and Burns (2012), and Oregon Geologic Data Compilation (OGDC), release 6 (Smith and Roe, 2015) (**Table 1; Figure 7**). The recent, highly detailed work by Ma and others (2012) was best suited to the needs of this study, because the work focused on mapping surficial units and it was prepared for applications similar to this one. The applicability of source data and the level of effort required to modify linework are summarized in **Table 1.**

We added three surficial units from other sources to our geologic maps. These data were given precedence over data from the principal sources listed in **Table 1**. These additional units are glacial deposits (Qgd) from Burns and others (2015) in the Bull Run Watershed, pyroclastic flow deposits (Qhpc) from Burns and others (2011) near Mount Hood, and fans (Qf) from SLIDO-3.4 (Burns and Watzig, 2017) across much of the study area. Although these units do not represent a large area, we used them because they are the best available sources of surficial unit mapping in their respective areas.

Table 1. Notes on quality and applicability of principal sources for geologic data.

Source	Priority	Notes on Quality and Applicability	Linework Changes
Ma and others (2012)	1	Geologic mapping focused on surficial deposits (such as loess), making it well suited to the needs of this study. Mapping was conducted at a 1:4,000 to 1:24,000 scale and was based on the most recent, 1-m lidar-derived topography available.	No linework changes required. The unit boundaries matched surficial units visible in the lidar topography.
Wells and others, (unpub. data, 2017)	2	Geologic mapping did not focus on surficial deposits units and thus did not capture surficial units as consistently or in as great of detail as the work by Ma and others (2012). Mapping was conducted at a 1:24,000 scale; 13 of the 51 quadrangles included in this study were mapped or remapped using lidar-derived topography.	Some linework changes required to match surficial units visible in the lidar topography. Linework modifications were concentrated in more densely populated areas and along major transportation networks, as these are key areas for accurately estimating risk and potential damage.
Mickelson and Burns (2012)	3	Very basic surficial geology; created as part of a landslide mapping study for Clatskanie, Oregon. Landslide units were mapped to lidar data at a scale of 1:4,000, but other geologic units were mapped at resolutions up to 1:24,000; some linework amendments were needed.	Some linework changes required to match surficial units visible in the lidar topography.
OGDC-6 (Smith and Roe, 2015)	4	Compilation of a wide range of past mapping efforts including professional papers, interpretive maps, special papers, and open-file reports from the USGS, DOGAMI, and Washington Department of Natural Resources, as well as student theses. Publication dates range from 1978 to 2004. Data in these studies were mapped onto base maps from as early as the 1950s, at scales ranging from 1:24,000 to 1:500,000. Because these maps were developed by dozens of different authors for a wide range of purposes, datasets vary in quality and applicability to this report.	Some linework changes required to match units to visible lidar boundaries. Most changes focused on reshaping existing units, but some new digitization of specific active or recent river deposits was required. Linework modifications were concentrated in more densely populated areas and along major transportation networks, because these are key areas for accurately estimating risk and potential damage.

Figure 7. Principal sources of geologic data for the study area. Figure does not show minor contributions from Burns and others (2015), Burns and others (2011), and SLIDO-3.4 (Burns and Watzig, 2017).

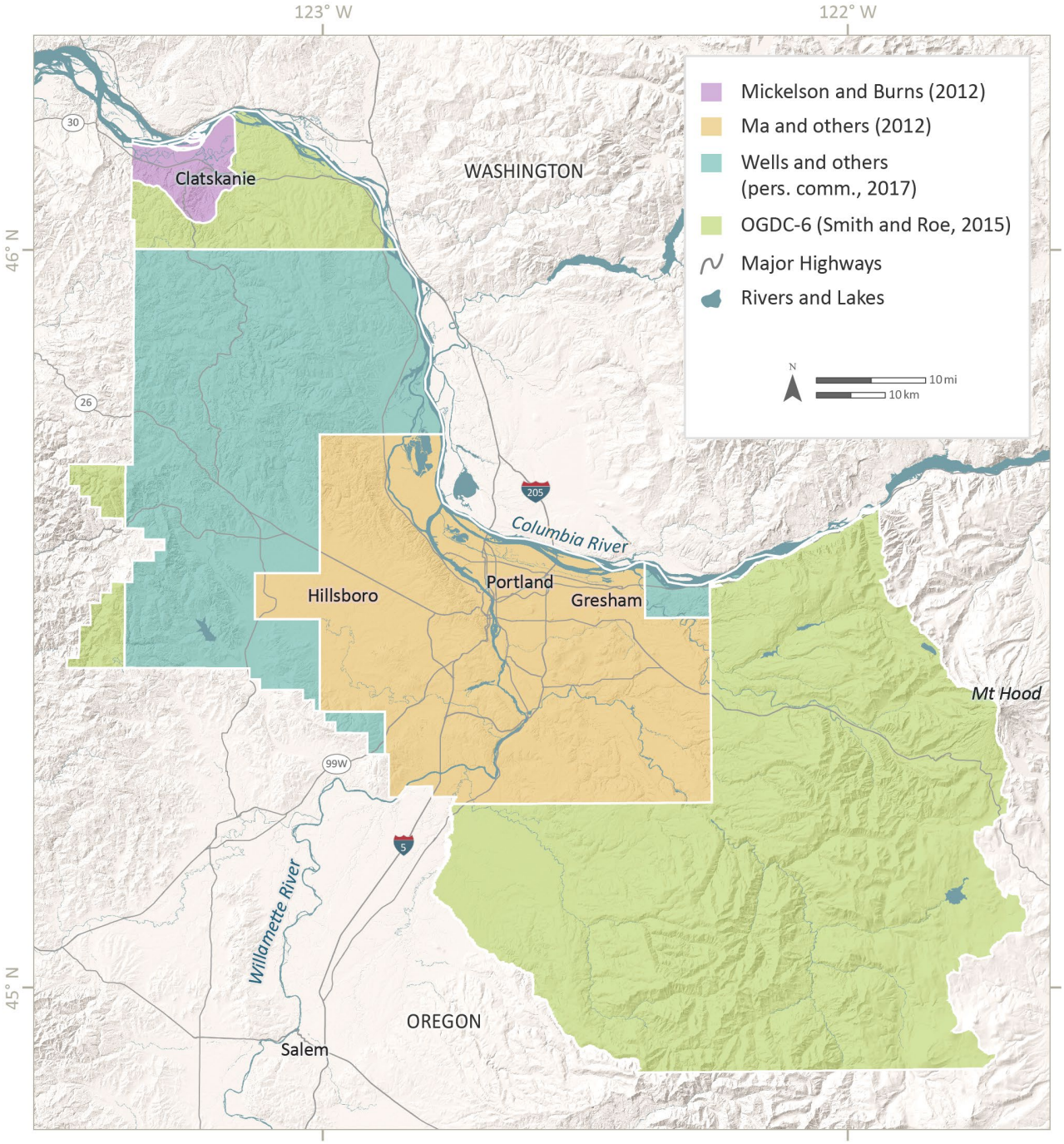

After creating a compilation of the geologic maps best suited to our study, we used GIS software to remove all landslide units from the compilation geologic map and replace them with our interpretation of the underlying geologic units. We did this for all landslide units listed in **Table 2**. If a mapped landslide was surrounded completely by a single geologic unit, we assumed that that single unit was under the entire landslide. For landslides that crossed multiple geologic units, we interpreted a combination of those geologic units to underlie the landslide, and we digitized geologic contacts based on nearby geologic contacts and topographic patterns (**Figure 8**). We drew these contacts at a scale of 1:4,000 or finer.

Figure 8. Example of interpreted geologic unit contacts underlying mapped landslides.

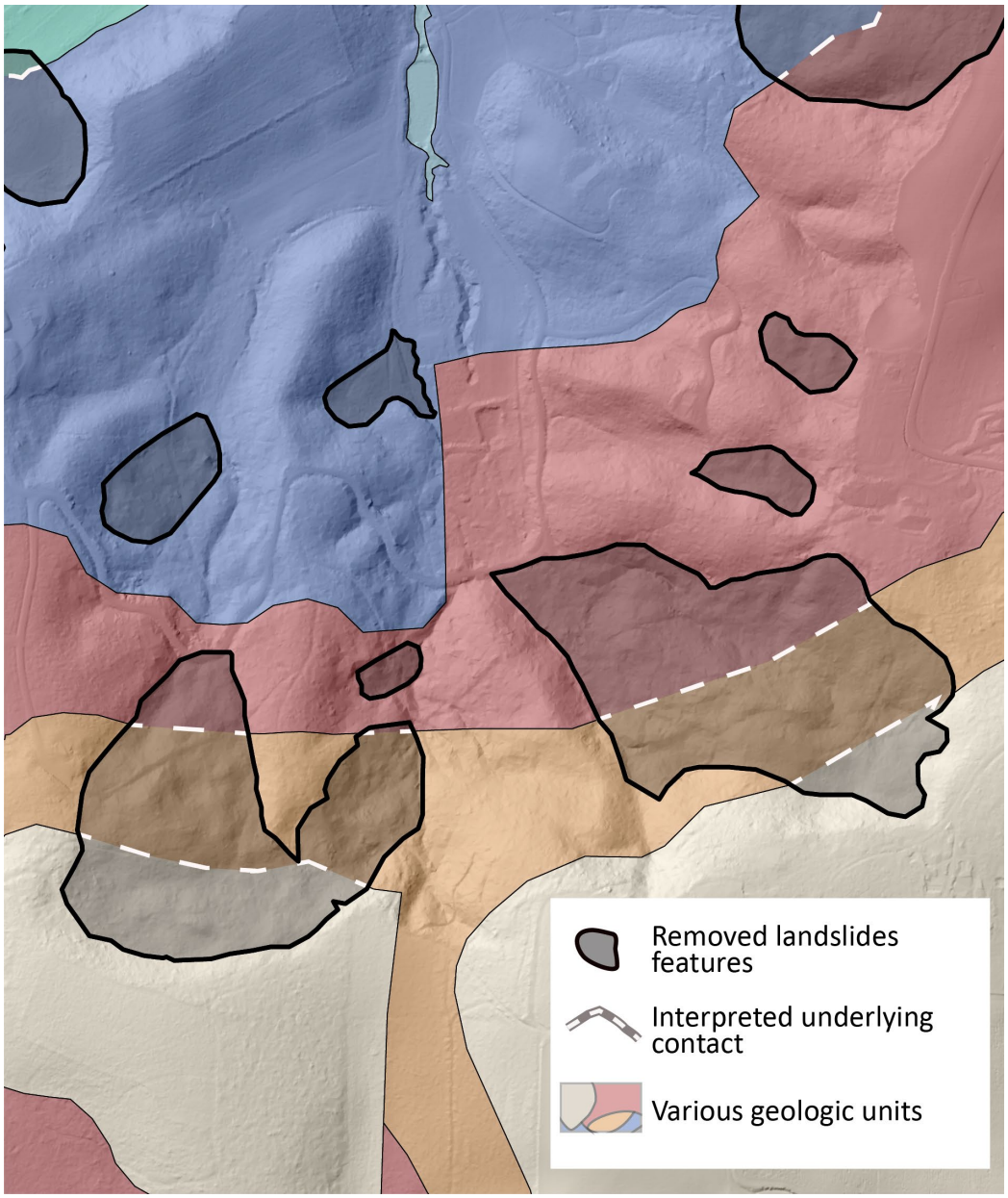

Table 2. Landslide units removed from geologic maps.

Source	Removed Landslide Units
Ma and others (2012)	Als (Recent or active landslide deposits) Qls (Landslide deposits) Qlww (Wildwood Landslide Complex) Qld (Dutch Canyon Landslide Complex) Qf (Debris flow fans) Qof (Older fan and colluvial deposits)
R. Wells and others (unpub. data, 2017)	Qls (Landslide deposits) Qlso (Older Landslide Deposits) Qt Talus
OGDC-6 (Smith and Roe, 2015)	Qls (Landslide, Landslide debris, Landslide deposits, Landslides) Ql (Landslide Deposits)
Mickelson and Burns (2012)	Landslide (deep)

After all landslide deposits had been removed from the geologic map, we reviewed map units and unit linework for adherence to features visible in the lidar-derived topography and consistency across map boundaries. Due to differing qualities in base maps, we found substantial inconsistencies, particularly in the surficial map units of R. Wells and others (unpub. data, 2017) and OGDC-6 (Smith and Roe, 2015). Resolving these issues required several steps. First, we first digitized or modified alluvium, colluvium, water bodies, and river terraces in areas where little or no surficial mapping had been previously completed. We added fan deposits from SLIDO-3.4 (Burns and Watzig, 2017) back to the geologic map. We also used the most recent available data from Natural Resources Conservation Service soil maps (2018) as an additional visual reference for modifying linework in areas where no recent lidar-based surficial geologic mapping was available. These units were digitized at a scale of 1:10,000 or finer using the most recent 1-m lidar imagery. **Figure 9** and **Table B-13** list the acquisition dates for the lidar data used by this study; these dates range from 2004 to 2015. Lidar basemap imagery was not available for the entire study area, but this was not a limitation in this study because our linework changes focused on areas with buildings and major transportation networks that had lidar coverage. The gaps in the lidar coverage are primarily in areas of southeastern Clackamas County, which have a relatively low population density compared the overall study area. Second, we amended geologic map unit boundaries from these sources to make a seamless boundary. Third, there were abundant GIS topological errors (including polygons gaps and overlapping slivers) within the map units from OGDC-6. We corrected many of these errors by closing gaps and removing slivers from the dataset to create a more uniform final product.

Figure 9. Lidar acquisition dates for study area. See Table B-13 for a list of lidar datasets.

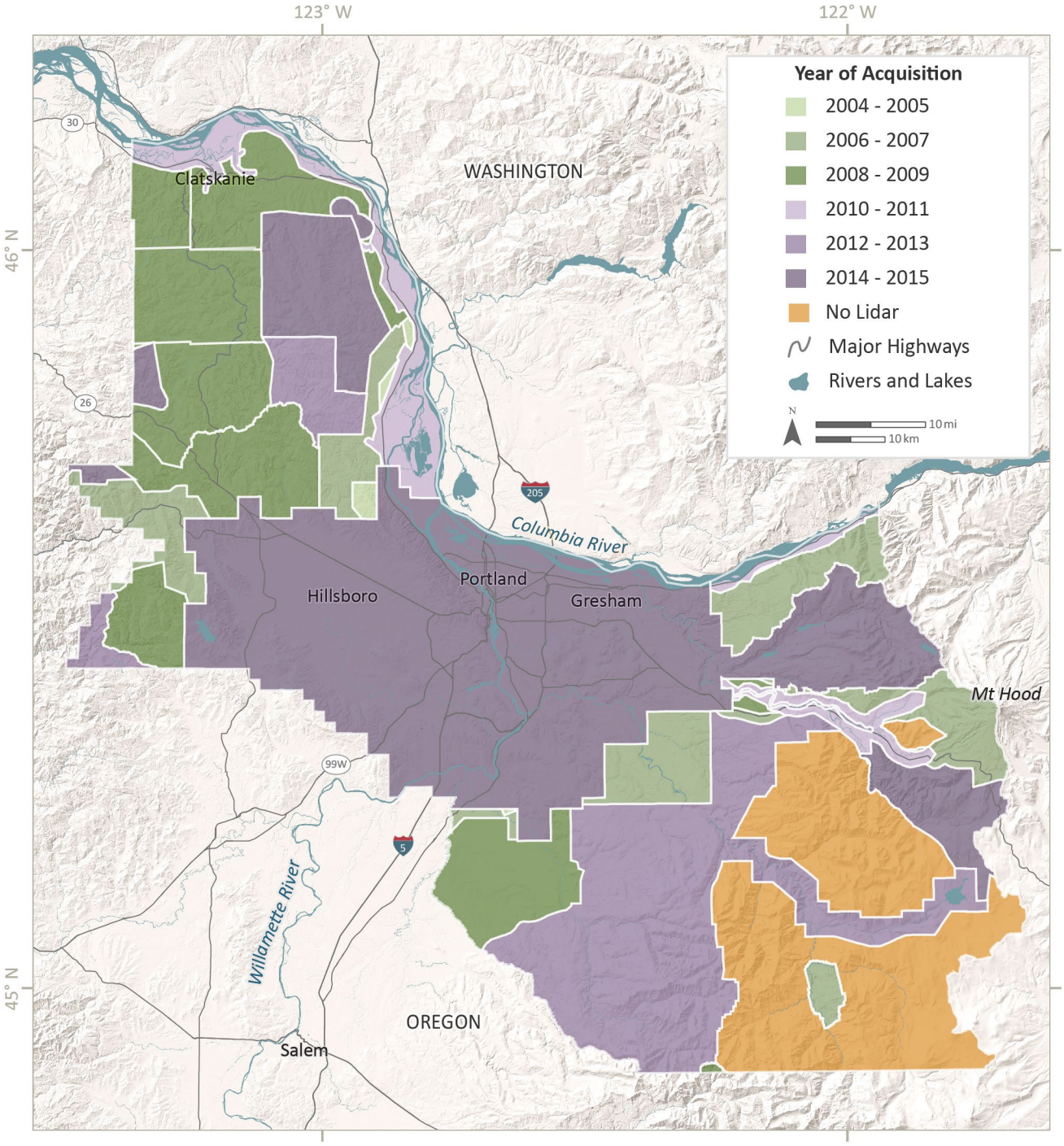

Once GIS linework corrections were complete, we used a copy of the unified geologic map without landslides for the liquefaction susceptibility map (section **3.5**). On another copy of the geologic map we superimposed a compilation of landslides across the entire study area. The landslide data we used in the compilation is discussed in Section **3.3** and includes both new mapping and mapping from SLIDO-3.4 (Burns and Watzig, 2017) and from R. Wells and others (unpub. data, 2011). From SLIDO-3.4, we included

the units mapped as landslides, fans, and talus (Qls) as well as pyroclastic deposits (Qhc, Qhoc, Qhpc, Qhtc). A final copy of the geologic map with landslides was retained for use in creating the landslide susceptibility and soil amplification class maps.

3.3 Landslide Susceptibility

To produce landslide susceptibility maps for "wet" and "dry" groundwater conditions, we followed the coseismic landslide susceptibility method of Wilson and Keefer (1985) and Wieczorek and others (1985) outlined in Hazus technical manual (FEMA, 2011). Using this method, landslide susceptibility is classified using a scale from none to 10 (11 classes). As shown in **Table 3**, three factors determine the final landslide susceptibility class: 1) wet or dry groundwater conditions, 2) terrain slope angle, and 3) geologic materials. Within this conceptual framework there are two possible scenarios: the ground is either "wet," that is, fully saturated, up to and including the surface of the ground or landslide, or "dry," that is, the top of the water table is beneath the landslide mass (**Table 3**). We modeled both scenarios in this study. To account for variations in terrain slope, we created an initial slope raster from the best available digital elevation model (DEM) (**Figure 9**). We resampled the DEM from 3-ft cells to 10-ft cells using the mean of the neighboring cells in order to remove or reduce very small (low relief) slope features. We then reclassified the slope raster into six classes from 0 to >40 degrees in accordance with the Hazus methodology (**Table 3**).

Table 3. Landslide susceptibility for (a) dry and (b) wet conditions (FEMA, 2011, Table 4.15).

		Slope Angle, degrees					
	Geologic Group	**0–10**	**10–15**	**15–20**	**20–30**	**30–40**	**>40**
	(a) Dry (groundwater below level of sliding)						
A	Strongly Cemented Rocks (crystalline rocks and well-cemented sandstone, c' = 300 psf, ϕ' = 35°)	none	none	I	II	IV	VI
B	Weakly Cemented Rocks (sandy soils and poorly cemented sandstone, c' = 0, ϕ' = 35°)	none	III	IV	V	VI	VII
C	Argillaceous Rocks (shales, clayey soil, existing landslides, poorly compacted fills, c' = 0, ϕ' = 20°)	V	VI	VII	IX	IX	IX
	(b) Wet (groundwater level at ground surface)						
A	Strongly Cemented Rocks (crystalline rocks and well-cemented sandstone, c' = 300 psf, ϕ' = 35°)	none	III	VI	VII	VIII	VIII
B	Weakly Cemented Rocks (sandy soils and poorly cemented sandstone, c' = 0, ϕ' = 35°)	V	VIII	IX	IX	IX	X
C	Argillaceous Rocks (shales, clayey soil, existing landslides, poorly compacted fills, c' = 0, ϕ' = 20°)	VII	IX	X	X	X	X

The geotechnical characteristics that influence the landslide susceptible geologic groups are divided into three sets (**Table 3**): A) Strongly Cemented Rocks, B) Weakly Cemented Rocks and Soils, and C) Argillaceous Rocks. These factors relate to the unit's general geotechnical properties such as strength, but also to depositional setting and unit history. Group C includes existing landslides. Existing landslides are an important factor in where future landslides are likely to occur and in increasing an area's landslide susceptibility within the model. As shown in **Table 3**, regardless of terrain slope angle, areas mapped as existing landslides are automatically identified as having a susceptibility of V (dry) or VII (wet).

Because accounting for existing landslides is key to accurately predicting landslide susceptibility, we both compiled the best available landslide mapping and performed limited additional mapping for this study (**Figure 10**).

With the available funding and project needs, we chose to focus our new landslide inventory mapping in western Clackamas County (shown in yellow in **Figure 10**), eastern Columbia County (also shown in yellow), and along the southern boundary of Washington County (shown in orange). The greatest need for new mapping was determined by the location and density of buildings, permanent residents, infrastructure, and the quality of existing landslide data. In Clackamas and Columbia Counties, we mapped landslide deposits following a portion of DOGAMI Special Paper 42, *Protocol for Inventory Mapping of Landslide Deposits from Light Detection and Ranging (Lidar) Imagery* by Burns and Madin (2009) (SP-42). The SP-42 protocol established a peer-reviewed, standardized methodology for mapping landslides in Oregon at a scale of 1:10,000 or finer. Because of limited funding, we made the most efficient use of time by mapping landslide deposit boundaries according to the SP-42 protocol but not landslide head and flank scarps or attributes, and by mapping at a scale of 1:4,000 with a focus on more obvious, large, deep landslides. In Washington County, we completed SP-42 landslide mapping in the Gaston and Laurelwood quadrangles (shown in orange in **Figure 10**).

We compiled the best available landslide inventory data for the remainder of the study area into a single dataset. We ranked landslide datasets based on their level of quality and scale of mapping. High-quality datasets, such as the complete landslide inventory for Multnomah County that follows full SP-42 methodology, were given the highest ranking and superseded older, less detailed mapping. Thus, the best available dataset is always present at any location in the final GIS dataset.

Figure 10. Sources of landslide data.

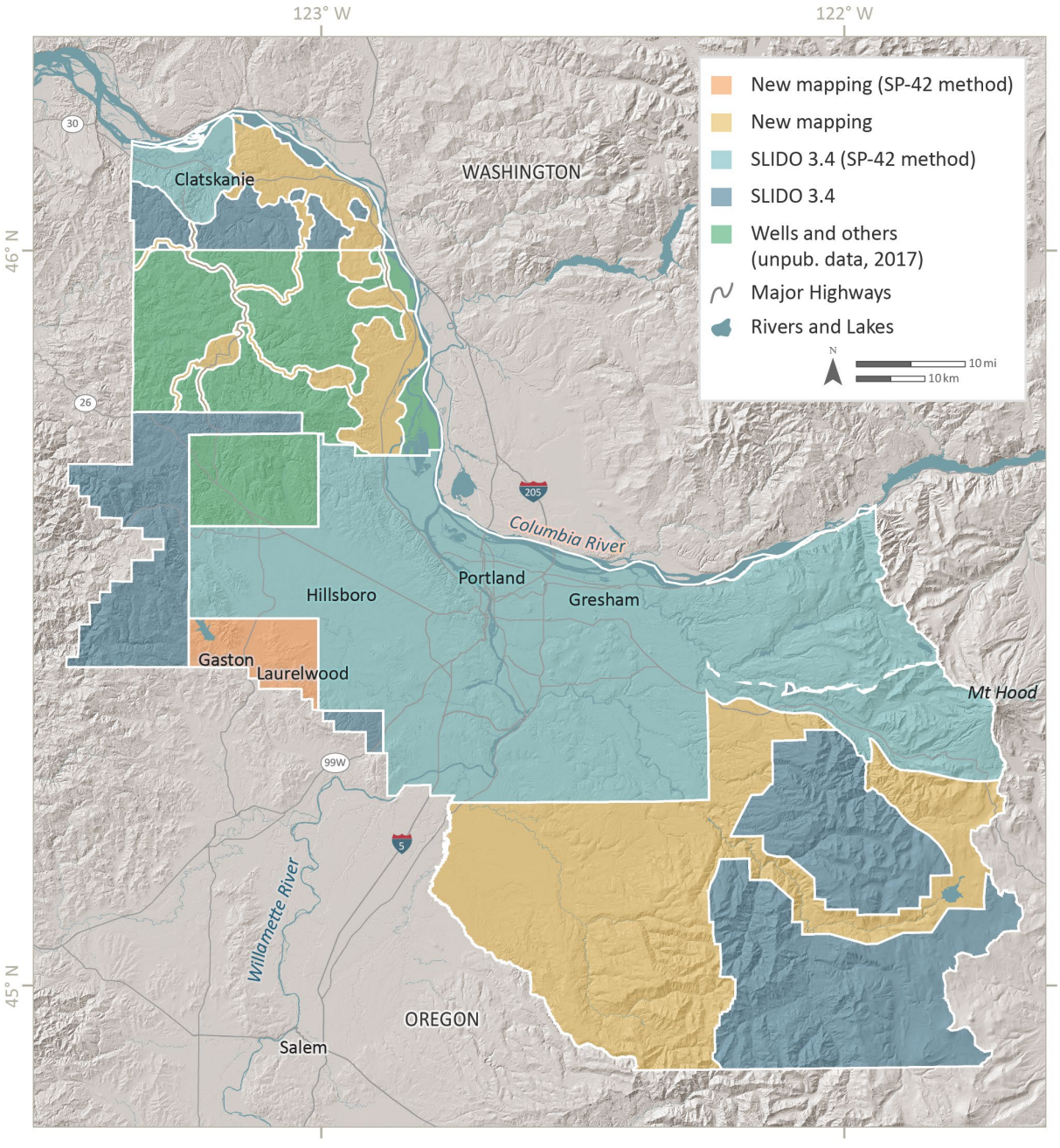

The final landslide inventory dataset was stamped into the final unified geologic map to create a unified geologic map with landslides (**Figure 6**). We then classified all units in this geologic map with landslides into one of three landslide geologic groups (A, B, C; see **Table 4**)—group A: Volcanic Bedrock; group B: Alluvium, Missoula Flood Deposits, and Aeolian Deposits; group C: Artificial Fill, Colluvium, and Landslides as (**Table 4**).

Table 4. Generalized geologic unit type associated with landslide geologic groups.

Generalized Unit Type	Examples	Landslide Geologic Group
Aeolian Deposits	Pleistocene loess	B
Alluvium	Active channel beds and bars; recently or post-Missoula flood deposits; lacustrine deposits	B
Artificial Fill	Artificial fill	C
Colluvium	Unconsolidated deposits; talus	C
Landslides	Landslides, debris flows	C
Missoula Flood Deposits	Missoula flood deposits- coarse-grained facies	B
Missoula Flood Deposits	Missoula flood deposits - fine-grained facies	B
Sedimentary Bedrock	Quaternary and Tertiary sedimentary rocks (e.g., members of Hillsboro Formation, Troutdale Formation, Scappoose Formation, etc.)	B
Volcanic Bedrock	Quaternary and Tertiary volcanic rocks (e.g. members of the Boring Volcanics, Grande Ronde Basalts, Siletz River Volcanics)	A

Several data limitations and methodology choices constrain the quality and applicability of the final maps. First, the DEM used to create the slope dataset was created with several different lidar-derived datasets and the National Elevation Dataset (NED) (**Figure 9**). This results in a range of quality across the study area (**Figure 9**). The source geologic and landslide datasets we used in the study were created for different purposes at different times, are based on diverse topographic data, and were mapped at different scales. As a result, source maps and subsequent soil amplification maps vary and can change abruptly across the study area. Time constraints on the study did not allow for fieldwork to resolve these artifacts. These maps were developed to support a regional analysis of landslide susceptibility maps and cannot replace site-specific examination.

The quality of landslide mapping varied based on source methodology and lidar availability. As shown in **Figure 10**, many sources followed the methodology developed in SP-42 (Burns and Madin, 2009). Landslide mapping following the SP-42 protocol is considered very high quality and is prioritized in this study over landslide mapping that did not follow SP-42. The landslides provided by R. Wells and others (unpub data, 2011) followed the initial polygon creation steps outlined in SP-42 and have greater detail than the landslides shown in the geologic map by R. Wells and others (unpub. data, 2017).

3.4 Soil Amplification Class

To create the soil amplification class map, we categorized all geologic units (including landslides) into one of six classes developed by the National Earthquake Hazard Reduction Program (NEHRP) (Buildings Seismic Safety Council, 1997; FEMA, 2003). The six NEHRP classes are divided into Hard Rock (type A), Rock (type B), Very Dense Soil and Soft Rock (type C), Stiff Soils (type D), Soft Soils (type E), and Soils Requiring Site-Specific Evaluations (type F). NEHRP classes are defined by the average speed at which a shear wave propagates through the upper 30 m (98 feet) of a unit (abbreviated as Vs30). Shear wave velocity is widely recognized as a key parameter for quantifying the behavior of soil in the shallow subsurface and is commonly used in seismic building guidelines (Buildings Seismic Safety Council, 1997). **Table 5** is a reproduction from FEMA (2003) showing the NEHRP classes by Vs30.

Table 5. NEHRP site classes (Buildings Seismic Safety Council, 1997, p. 33, as modified by FEMA, 2003).

Site Class	Site Class Description	Shear Wave Velocity (m/s) Min.[1]	Shear Wave Velocity (m/s) Max.[1]	DOGAMI Hazard Class
A	Hard Rock	1500	—	very low
B	Rock	760	1500	low
C	Very Dense Soil and Soft Rock. $s_u \geq 2{,}000$ psf (100 kPa) or $N > 50$ [1]	360	760	moderate
D	Stiff Soils (stiff soil with undrained shear strength). 1,000 psf $\leq s_u \leq$ 2,000 psf (50 kPa $\leq s_u \leq$ 100 kPa) or $15 \leq N \leq 50$ [1]	180	360	high
E	Soft Soils. Profile with more than 3 m of soft clay defined as soil with PI > 20, moisture content w > 40%, and undrained shear strength $s_u <$ 2,000 psf (50 kPa) or $N < 15$ [1]	—	180	very high*
F	Soils Requiring Site-Specific Evaluations: 1. Soils vulnerable to potential failure or collapse under seismic loading such as liquefiable soils, quick and highly sensitive clays, collapsible weakly cemented soils. 2. Peat and/or highly organic clays (H > 3 m of peat and/or highly organic clay) [1] 3. Very high plasticity clays (H > 8 m with PI > 75) [1] 4. Very thick, soft/medium stiff clays (H > 36 m) with $s_u <$ 1,000 psf (50 kPa) [1]	—	—	*requires site-specific evaluation*

[1] Min. is minimum, Max. is maximum, s_u is undrained shear strength; *N* is Standard Penetration Test blow count; PI is plasticity index; H is soil thickness.

We mapped soil amplification class throughout in study area by assigning NEHRP classes to the surficial lithologies in the unified geologic map that included landslides. Assignments were informed by Roe and Madin's (2013) shear wave velocity modeling for the Portland metropolitan area (**Table 2**, **Table 4**). This modeling was informed by 3D physical models of the surficial and near-surface geologic units based on previous mapping efforts (including the compiled maps of Ma and others [2012]) as well as geotechnical data from more than 8,000 drill holes and more than 200 shear wave velocity survey points. NEHRP class assignments were also informed by geologic unit descriptions. We classified units into soil amplification classes based on deposit characteristics such as deposit density, cementation, and cohesion

As summarized in **Table 6,** areas composed of older, Tertiary volcanic bedrock judged to have thin or no soil accumulation in the eastern half of the study area were classified as "low" hazard for soil amplification (class B). We classified regions with coarse-grained Missoula flood deposits, or sedimentary or volcanic bedrock as moderate hazard (class C). We classified regions dominated by older alluvium, fine-

grained Missoula flood deposits, Pleistocene loess, or loess mixed with bedrock as high hazard (class D). Very recent alluvial deposits and lacustrine environments were classified as very high hazard (class E). No areas were determined to have very low (class A) hazard for soil amplification, which is typical in the west coast of the United States.

Table 6. Generalized geologic unit type associated with NEHRP classes.

Generalized Unit Type	Examples	NEHRP Class
Aeolian Deposits	Pleistocene loess	D
Aeolian Deposits	Floodplain dune deposits	E
Alluvium	Older, finer-grained fluvial deposits and river terraces; pre-Missoula flood deposits	D
Alluvium	Active channel beds and bars; recently or post-Missoula flood deposits; lacustrine deposits	E
Artificial Fill	Artificial fill	F
Colluvium	Unconsolidated deposits; talus	F
Landslides	Landslides, debris flows	F
Missoula Flood Deposits	Missoula flood deposits- coarse-grained facies	C
Missoula Flood Deposits	Missoula flood deposits - fine-grained facies	D
Sedimentary Bedrock	Quaternary and Tertiary sedimentary rocks (e.g. members of Hillsboro Formation, Troutdale Formation, Scappoose Formation, etc.)	C
Sedimentary Bedrock with Loess	Quaternary and Tertiary sedimentary rocks with loess	D
Volcanic Bedrock	Columbia River Basalts bedrock with thin to no soil	B
Volcanic Bedrock	Quaternary and Tertiary volcanic rocks (e.g. members of the Boring Volcanics, Grande Ronde Basalts, Siletz River Volcanics)	C
Volcanic Bedrock with Loess	Quaternary and Tertiary volcanic rocks with loess	D
Water	Lakes, Rivers	E
Water	Ice	C

Areas composed of artificial fill, landslides, and unconsolidated deposits were classified as F, given that they require site-specific analysis. These units may be highly complex, heterogenous soils that may have experienced ground movement or liquefaction. Because site-specific analysis was not within the scope of the project and the Hazus model is unable to process class F units, as they have a wide range of soil amplification potential. Bauer and others (2018) chose to conservatively reclassify class F units as class E when running their analysis.

Several data limitations and methodology choices constrain the quality and applicability of the final map. First, the geologic and landslide datasets we used in the study were created for different purposes at different times, are based on diverse topographic data, and were mapped at different scales. As a result, source maps and subsequent soil amplification maps vary and can abruptly change across the study area.

Second, we assumed that the geologic units on our map compilation represented the upper 30 m (98 feet) of surficial material. We recognize that this may not be the case in some areas and may lead to more conservative soil amplification predictions (i.e., more intense shaking) where better data are not available. Third, the work in this study had time constraints that did not allow for a methodical field assessment. We emphasize that these maps were developed to support a regional analysis of soil amplification classes and cannot replace site-specific examination.

3.5 Liquefaction Susceptibility

To create our liquefaction susceptibility map, we categorized all geologic units into one of six qualitative classes developed by Youd and Perkins (1978) and used by Hazus (FEMA, 2011). These susceptibility

classes include none, very low, low, moderate, high, and very high; in Hazus, they are labeled 0 to 5, respectively. Hazus uses these classes to determine which coefficients to use to calculate liquefaction probability. We did not include landslide units in our liquefaction susceptibility mapping as Hazus accounts for the impact of landslides on ground deformation as a separate input.

Although sediment saturation and amplitude and duration of ground shaking are key factors in initiating soil liquefaction, our liquefaction mapping potential did not directly consider them because Hazus includes these factors as separate inputs to its model (FEMA, 2011). When Bauer and others (2018) performed their analysis of earthquake damage using the liquefaction data produced by this report, they modeled several different scenarios including one in which all soils were assumed to be fully saturated and another in which all soils were unsaturated. The liquefaction maps presented here reflect the liquefaction susceptibility based on only unit lithology and not on the water table, thus are appropriate as an input for Hazus modeling.

Lithological characteristics that influence liquefaction susceptibility that we considered when reviewing unit descriptions included consolidation, cementation, cohesion, sorting, depth, grain size, density, and grain shape. These factors closely relate to the unit's age, depositional process, and unit history. Because of these relationships, Youd and Perkins (1978) provide guidelines and a table of examples of sedimentary deposits with liquefaction susceptibility classes, organized by unit age, deposit type, and distribution of cohesionless sediments within the deposit. This table is reproduced as **Table 7**. We used this Youd and Perkins (1978) rating system for guidance in making our liquefaction susceptibility assignments.

We used data from an assessment by Fugro Consultants (unpub. data., 2015) that identified peak ground acceleration thresholds that triggered liquefaction for six sampled geologic units in the Portland area (Quaternary alluvium, artificial fill, coarse-grained Missoula flood deposits, fine-grained Missoula flood deposits, loess, and landslides). We compared these thresholds to the thresholds listed for each Hazus liquefaction susceptibility class (FEMA, 2011, Table 4.13) and used the local data to refine the Youd and Perkins (1978) classifications (**Table 7**).

Table 7. Liquefaction susceptibility rating systems (from Youd and Perkins, 1978).

Type of Deposit	General Distribution of Cohesionless Sediments in Deposits	Likelihood That Cohesionless Sediments When Saturated, Would Be Susceptible to Liquefaction (by Age of Deposit)			
		Modern < 500 yr	Holocene < 11 ka	Pleistocene 11 ka - 2 Ma	Pre-Pleistocene > 2 Ma
Continental Deposits					
River channel	locally variable	very high	high	low	very low
Flood plain	locally variable	high	moderate	low	very low
Alluvial fan and plain	widespread	moderate	low	low	very low
Marine terraces and plains	widespread	—	low	very low	very low
Delta and fan-delta	widespread	high	moderate	low	very low
Lacustrine and playa	variable	high	moderate	low	very low
Colluvium	variable	high	moderate	low	very low
Talus	widespread	low	low	very low	very low
Dunes	widespread	high	moderate	low	very low
Loess	variable	high	high	high	unknown
Glacial till	variable	low	low	very low	very low
Tuff	rare	low	low	very low	very low
Tephra	widespread	high	high	?	?
Residual soils	rare	low	low	very low	very low
Sebka	locally variable	high	moderate	low	very low
Coastal Zone					
Delta	widespread	very high	high	low	very low
Estuarine	locally variable	high	moderate	low	very low
Beach					
—high wave energy	widespread	moderate	low	very low	very low
—low wave energy	widespread	high	moderate	low	very low
Lagoonal	locally variable	high	moderate	low	very low
Fore shore	locally variable	high	moderate	low	very low
Artificial					
Uncompacted fill	variable	very high	—	—	—
Compacted fill	variable	low	—	—	—

As summarized in **Table 8**, areas along rivers, floodplains, and valleys are typically classified as having Moderate, High, or Very High susceptibility to liquefaction. The active channel and recent deposits of the major rivers within the study area, including the floodplains of the Willamette, Columbia, Tualatin, and Clackamas Rivers, are classified as Very High, and older river terraces and alluvial deposits are classified as Moderate or High. We classified units mapped as unconsolidated colluvium including glacial deposits, talus, and pyroclastic flow deposits as Low or Moderate. We classified Artificial fill as Very High liquefaction susceptibility.

Table 8. Generalized geologic unit type associated with liquefaction susceptibility class.

Generalized Unit Type	Examples	Hazus Liquefaction Class	Relative Susceptibility
Aeolian Deposits	Pleistocene loess	4	High
Aeolian Deposits	Floodplain dune deposits	3	Moderate
Alluvium	Active channel beds and bars; very recent alluvial deposits	5	Very High
Alluvium	Post-Missoula flood deposits; recent river terraces; lacustrine deposits	4	High
Alluvium	Older alluvial deposits; high and weathered river terraces	3	Moderate
Alluvium	Pre-Missoula flood deposits	2	Low
Artificial Fill	Artificial fill	5	Very High
Colluvium	Pyroclastic flow and debris-flow deposits	3	Moderate
Colluvium	Talus; glacial deposits	2	Low
Missoula Flood Deposits	Missoula flood deposits - fine-grained facies	3	Moderate
Missoula Flood Deposits	Missoula flood deposits - coarse-grained facies	2	Low
Sedimentary Bedrock	Quaternary and Tertiary sedimentary rocks (e.g. members of Hillsboro Formation, Troutdale Formation, Scappoose Formation, etc.)	0	None
Sedimentary Bedrock with Loess	Quaternary and Tertiary sedimentary rocks with loess	3	Moderate
Volcanic Bedrock	Quaternary and Tertiary volcanic rocks (e.g. members of the Boring Volcanics, Grande Ronde Basalts, Siletz River Volcanics)	0	None
Volcanic Bedrock with Loess	Quaternary and Tertiary volcanic rocks with loess	3	Moderate
Water	Lakes, Rivers	5	Very High
Water	Snow and ice	2	Low

The bedrock-dominated areas of the Coastal Range and Cascade Mountains are much less likely to be susceptible to liquefaction and as such are classified as None. However, we classified areas with a documented mix of loess and bedrock as Moderate and regions mapped as dominantly loess as High based on evidence from Fugro Consultants (unpub. data, 2015).

Many of the geologic maps we relied upon in this study did not describe some key characteristics such as sediment cohesion or density that would be most useful in determining liquefaction potential. As a result, to classify geologic units we frequently relied on the Youd and Perkins (1978) depositional environment classification scheme, as well as inferences from the geologic mapping unit descriptions, and our regional knowledge of the units and area. We completed limited field reconnaissance work in Columbia County as time permitted. The majority of this work was to visually check alluvium and flood plain extents in relation to their spatial locations on lidar-derived imagery in a few populated centers of Columbia County.

As with the data and methodology limitations for soil amplification mapping, our liquefaction mapping efforts were constrained by variations in source map quality. The source geologic maps were originally created at different scales, for different purposes, and may not have used lidar-derived topographic imagery. In the absence of more complete data, we assumed the geologic units in our map compilation represented the upper 30 m (98 feet) of surficial material. We emphasize that we developed our data to support regional analysis of liquefaction potential, not site-specific examinations.

4.0 RESULTS

The results of the study are new GIS maps of soil amplification class, liquefaction susceptibility, and coseismic landslide susceptibility following the methods outlined in this paper and the Hazus Technical Manual and formatted for direct use in Hazus. More information regarding the use of these maps within Hazus can be found in **Appendix A.**

4.1 Soil Amplification Class

Figure 11 shows the soil amplification class map. The typical units and characteristics of these categories are displayed in **Table 6**; **Table B-1** through **Table B-4** show more detailed, unit-specific information with all classifications. The areas with higher likelihood of soil amplification are generally located along rivers and areas with a geologic history of river deposits. Artificial fill and landslides have been classified as soil amplification class F and appear as irregular blocks across the map.

The map shows that just over half of the land in the study area are soft rock and very dense soil, NEHRP class C ("moderate" soil amplification potential). These areas are primarily near the edges of Portland and the unincorporated extents of the four counties. The second most extensive classification are stiff soils, NEHRP class D ("high" soil amplification potential). These geologic units are concentrated within the Portland and Beaverton city limits. It is also worth noting that the areas with the highest potential soil amplification potential, soft soil geologic units (class E), are not as common but are can be found along historical floodplains including those of the Columbia River, Sauvie Island, and the Tualatin River and its tributaries.

Figure 11. Soil amplification class map of Clackamas, Columbia, Multnomah, and Washington Counties, Oregon.

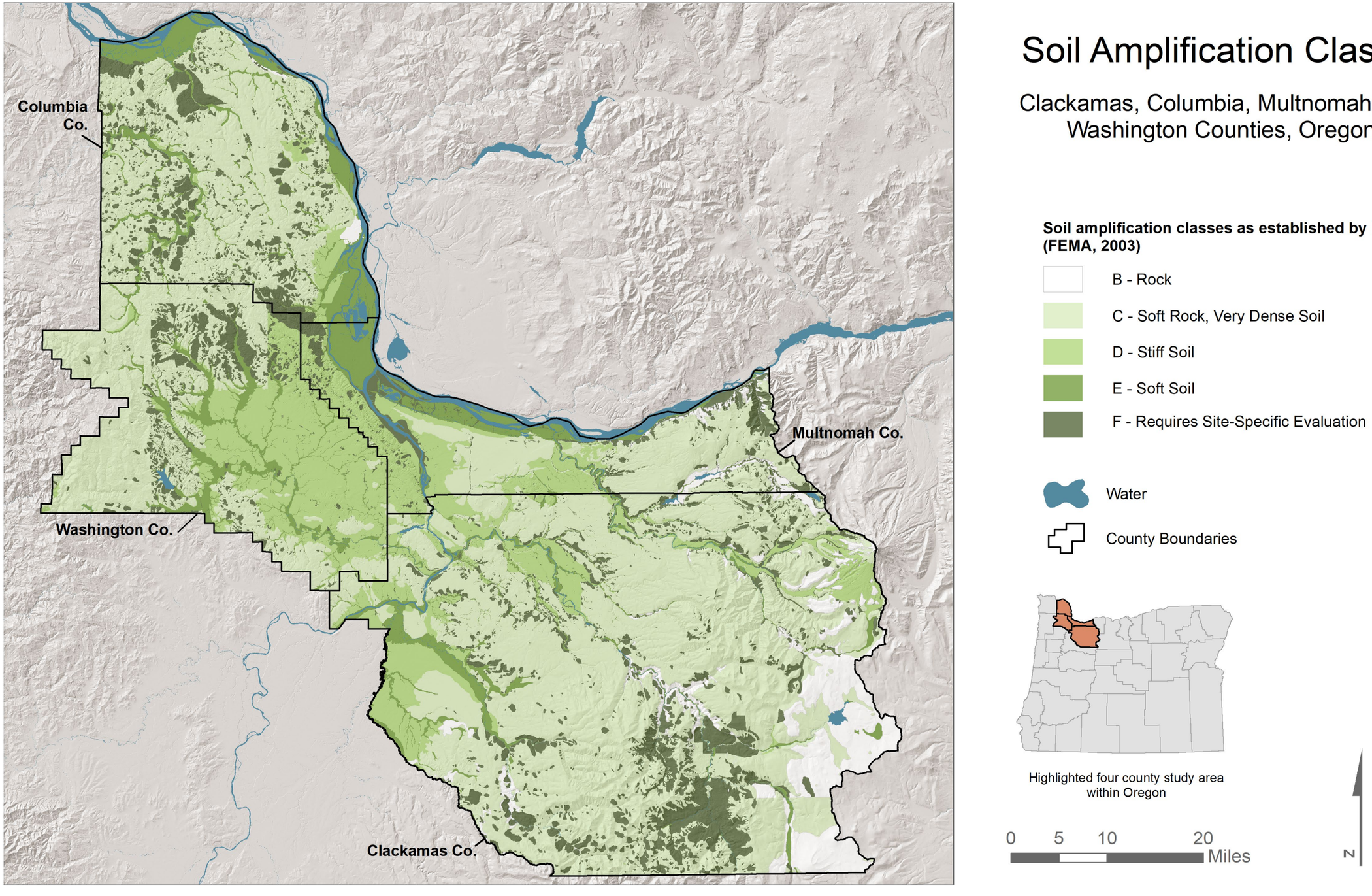

4.2 Liquefaction Susceptibility

Figure 12 shows the liquefaction susceptibility map. The typical units and characteristics of these categories are displayed in **Table 8**; **Table B-5** through **Table B-8** show more detailed, unit-specific information with all classifications. The areas with higher likelihood of liquefaction are generally located along the rivers and areas with a geologic history of river deposits. Artificial fill is assigned very high susceptibility and appears as irregular blocks across the map, often in former river valleys.

Figure 12 shows that about one third of the land in the study area is has Moderate or greater liquefaction susceptibility. The geologic units moderate or greater liquefaction susceptibility are mostly concentrated within the Portland metropolitan limits. Geologic units that have High susceptibility to liquefaction are not as common but can be found along historical floodplains including those of the Columbia River, Sauvie Island, the Tualatin River and its tributaries, the Sandy River, the Clackamas River, the Molalla River, the Pudding River, and the Willamette River.

Within the Hazus earthquake impact methodology, the liquefaction susceptibility classes (None to Very High) are associated with different coefficients used by Hazus to calculate the probability of liquefaction and the resulting permanent ground displacement for a given earthquake scenario. Under "worst case" conditions where earthquake magnitude, peak ground acceleration, and groundwater level are most conducive to liquefaction, the maximum probability of liquefaction for any site within each class is: ≤30.9% for Very High susceptibility; ≤24.7% for High susceptibility; ≤12.4% for Moderate susceptibility; ≤6.2% for Low susceptibility; and ≤2.5% for Very Low susceptibility (there are no Very Low areas in **Figure 12**). Liquefaction susceptibility will frequently be less than these "worst case" scenarios depending on the specific modeled earthquake magnitude, peak ground acceleration, and depth to groundwater. A more detailed explanation of the process used by Hazus to calculate probability of liquefaction is provided in **Appendix A**.

The susceptibility maps in this report can be used in combination with Hazus earthquake impact assessment results to understand potential risk, because the maps are key inputs to the Hazus earthquake model. For example, if a building or neighborhood is estimated to be severely damaged in the Hazus earthquake impact assessment, it would be prudent to review the maps produced by this report to determine if an area of interest has a relatively high potential risk from soil amplification, liquefaction, or landslides that would indicate the need for a site-specific, geotechnical analysis. Once the risk is better understood, appropriate mitigation actions could be taken.

Figure 12. Liquefaction susceptibility of Clackamas, Columbia, Multnomah, and Washington Counties, Oreg.

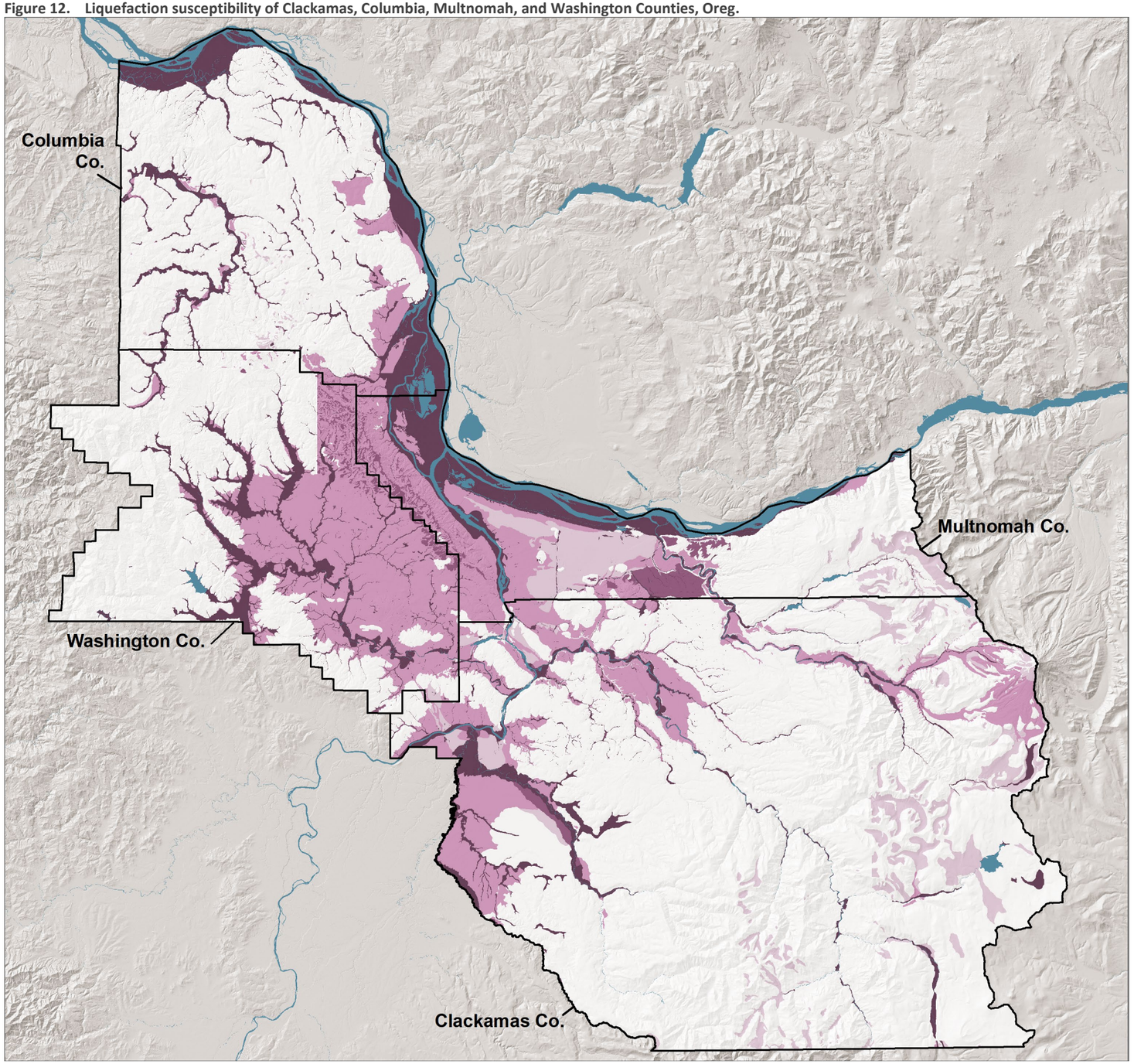

Liquefaction Susceptibility

Clackamas, Columbia, Multnomah, and Washington Counties, Oregon

Liquefaction Susceptibility

- None
- Low
- Moderate
- High
- Very High

Liquefaction susceptibility classes were created by categorizing geologic units into the six qualitative classes. The earthquake magnitude and groundwater were not considered in the creation of the susceptibility classes. However, the size of the earthquake and groundwater conditions at the time will have significant effects on the location and magnitude of liquefaction within each susceptibility class.

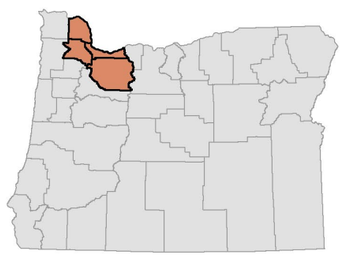

Highlighted four county study area within Oregon

- Water
- County Boundaries

0 5 10 20 Miles

N

4.3 Coseismic Landslide Susceptibility

Figure 13 and **Figure 14** show coseismic landslide susceptibility maps. The typical units and characteristics of these categories are displayed in **Table 4**; **Table** B-9 through **Table B-12** show more detailed, unit-specific information with all classifications. The areas with higher likelihood of coseismic landslides are generally located in the areas with greater relief and steeper slopes. Areas of existing landslides are more likely to move in future and thus appear on the map generally as irregular areas of the highest susceptibility classes.

The maps in **Figure 13** and **Figure 14** show that the land with the highest coseismic landslide susceptibility are spatially the inverse from those areas with higher potential soil amplification and liquefaction susceptibility. The areas with generally higher coseismic landslide susceptibility are in western Washington and Columbia Counties, along the Coast Range, in the central portion of the study area on slopes of the Tualatin Mountains, and in the eastern portion of the study area, along the Cascade Range.

The coseismic landslide susceptibility maps are based on geotechnical strength characteristics of the geologic units and slope steepness. Because groundwater conditions can have a significant effect on landslides, groundwater conditions are included as two scenarios (dry and wet) (**Table 3**). However, key factors required to induce landsliding, including earthquake magnitude and number of cycles of shaking, were not considered in the creation of the susceptibility classes. This means that under some circumstances, areas mapped as having a High coseismic landslide susceptibility (**Figure 13** and **Figure 14**) may not experience landsliding if the earthquake is too weak or too short in duration. Within the Hazus earthquake impact methodology, as with liquefaction, the landslide susceptibility classes (none to 10 [see **Table 3**]) are associated with different coefficients used by Hazus to calculate the probability of landsliding and the resulting permanent ground displacement for a given earthquake scenario.

These susceptibility maps can be used in combination with Hazus earthquake impact assessment results to understand potential risk, because they are key inputs to the Hazus earthquake model. For example, if a building or neighborhood is estimated to be severely damaged in the Hazus earthquake impact assessment, it would be prudent to review the maps produced by this report to determine if a specific area of interest has a relatively high potential risk from soil amplification, liquefaction, or landslide that would indicate the need for a site-specific, geotechnical analysis. Once the risk is better understood, appropriate mitigation actions could be taken.

Figure 13. Coseismic landslide susceptibility given dry groundwater conditions for Clackamas, Columbia, Multnomah, and Washington Counties, Oregon.

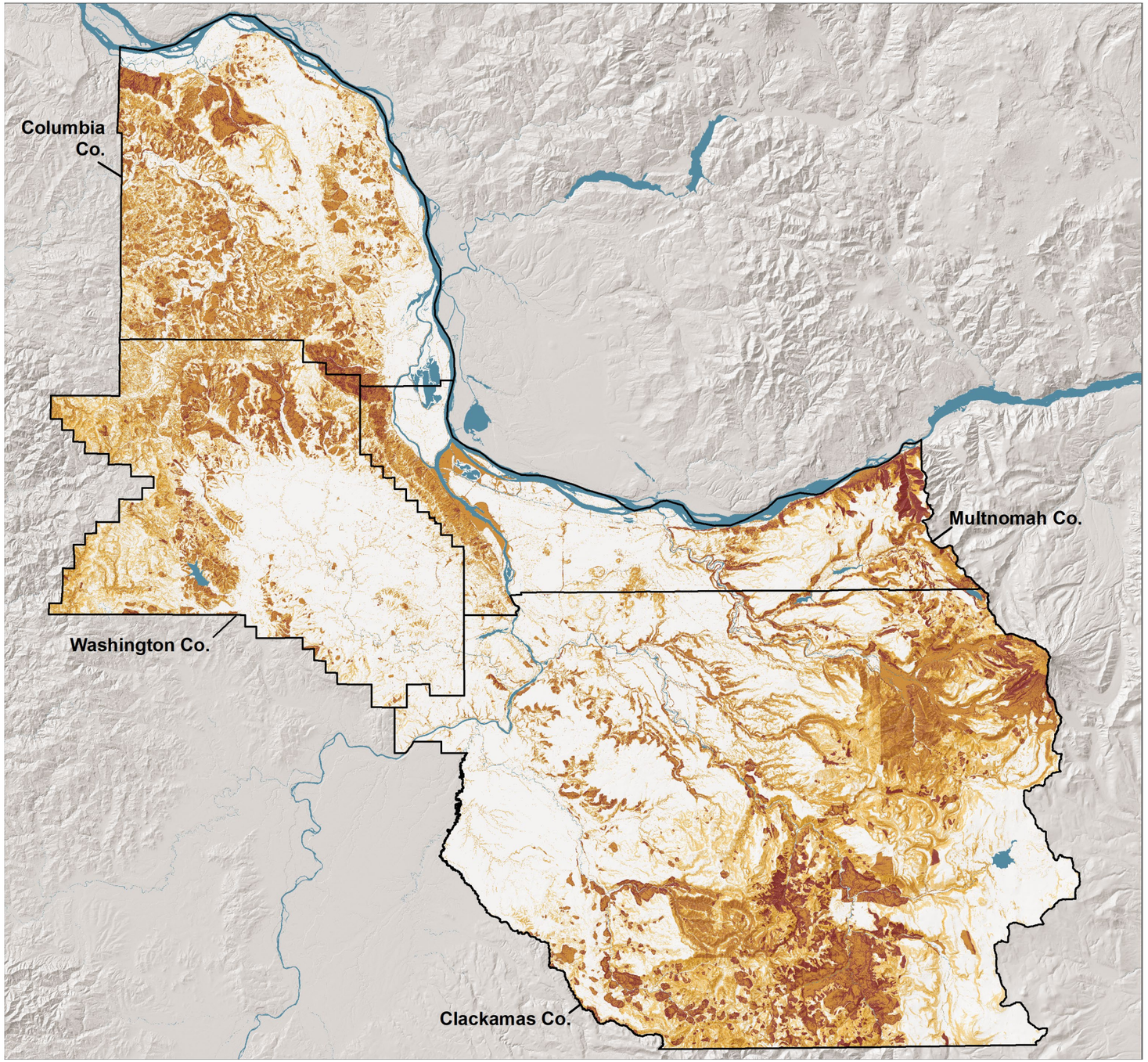

Coseismic Landslide Susceptibility (Dry)

Clackamas, Columbia, Multnomah, and Washington Counties, Oregon

Susceptibility of coseismic landslides during dry conditions

None (0) Low (1) High (9)

Landslide susceptibility classes were created by categorizing geologic units into eleven classes. The earthquake characteristics were not considered in the creation of the susceptibility classes. However, the size of the earthquake and number of cycles will have significant effects on the permanent ground displacement and ground failure.

Water

County Boundaries

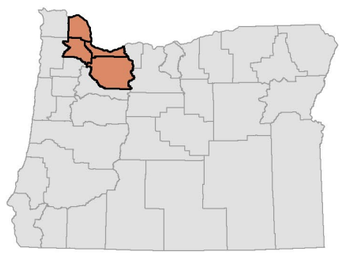

Highlighted four county study area within Oregon

0 5 10 20 Miles

N

Figure 14. Coseismic landslide susceptibility given wet groundwater conditions for Clackamas, Columbia, Multnomah, and Washington Counties, Oregon.

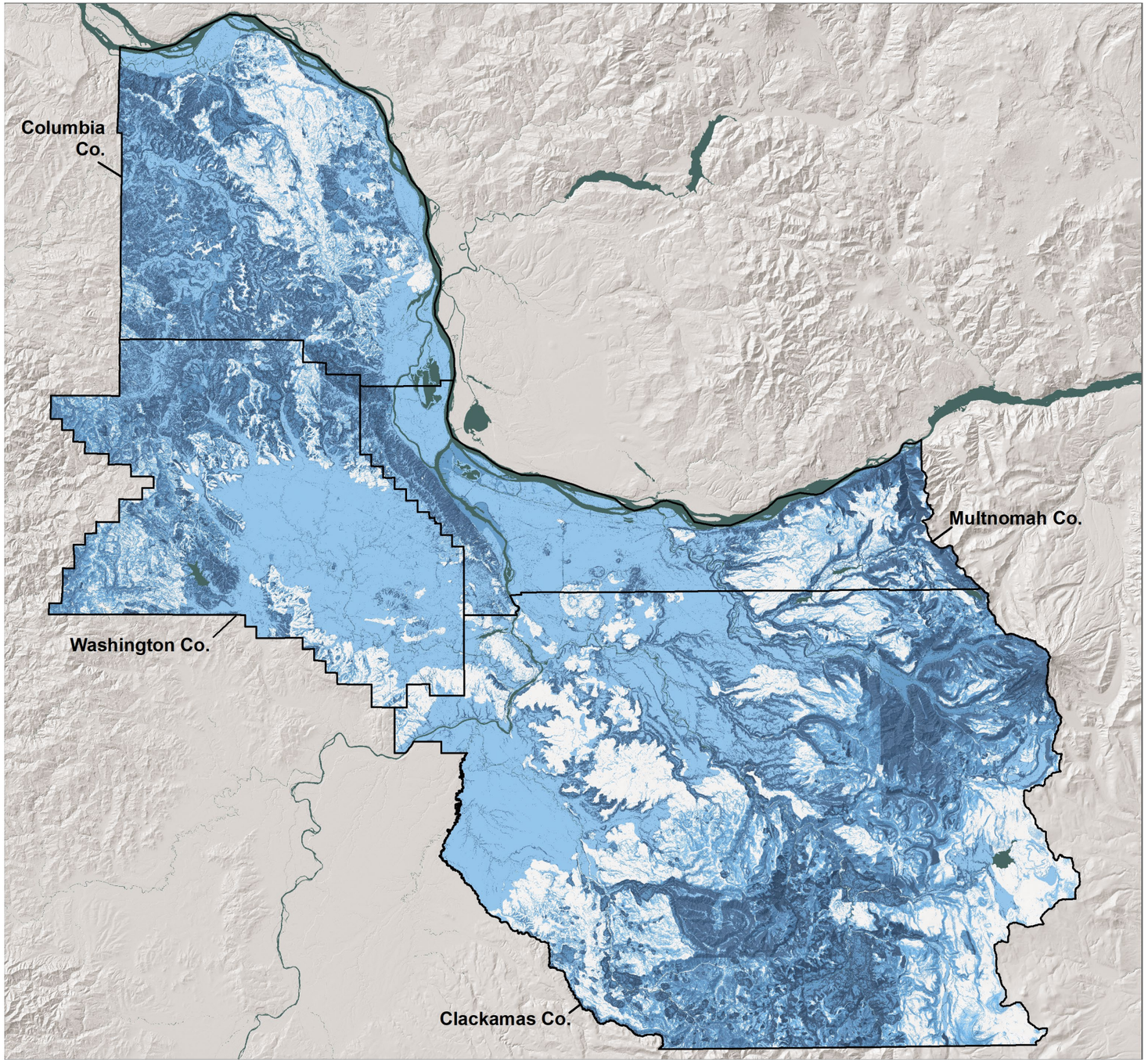

Coseismic Landslide Susceptibility (Wet)

Clackamas, Columbia, Multnomah, and Washington Counties, Oregon

Susceptibility of coseismic landslides during wet conditions

None (0) Low (1) High (10)

Landslide susceptibility classes were created by categorizing geologic units into eleven classes. The earthquake characteristics were not considered in the creation of the susceptibility classes. However, the size of the earthquake and number of cycles will have significant effects on the permanent ground displacement and ground failure.

Water

County Boundaries

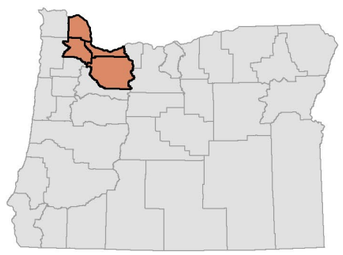

Highlighted four county study area within Oregon

0 5 10 20 Miles

N

5.0 DISCUSSION, CONCLUSIONS, AND RECOMMENDATIONS

The main purpose of this study was to create earthquake-induced hazards maps that can be used to help communities become more resilient to future earthquakes and coseismic hazards. These susceptibility maps include soil amplification, liquefaction, and coseismic landslides and were designed to be used to inform earthquake damage and loss models used in the assessment of Clackamas, Columbia, Multnomah, and Washington Counties (Bauer and others, 2018, J. Bauer, written commun., 2019). In addition, this report documents the methods used to create these maps and publishes the associated GIS data to make the information readily available. Although we cannot predict when future earthquake events will occur or how big they will be, this study improves our understanding of the geographic areas more likely to be impacted by future seismic hazards in a region of Oregon with relatively moderate to high seismic hazard.

The main factors influencing the spatially extensive coseismic hazards (liquefaction, soil amplification, and coseismic landslides) in the study area are: 1) a combination of relatively thick unconsolidated alluvium in valleys with relatively shallow regional groundwater and 2) an abundance of existing landslides, variable perched groundwater on the slopes (wet season and dry season), and weak rock and soil combined with steep slopes.

There are other key factors in evaluating coseismic hazards, such as identifying areas with existing landslides that are currently only marginally stable and can more easily become unstable if shaken. Historically, people have also moved and placed significant amounts of soil and rock termed "artificial fill," which if not properly engineered can perform very poorly if shaken.

Three primary conclusions of the project are:

- Areas of relatively thick unconsolidated alluvium in the valleys will likely result in amplification of the ground shaking. This will likely contribute to more damage in these areas, unless mitigation has been performed.
- Extensive areas of unconsolidated, non-cohesive soils are more likely to experience liquefaction. Approximately one third of the study area has a Moderate, High, or Very High liquefaction susceptibility classification based solely on the underlying geology. If an earthquake occurs during the wet season, there will be more liquefaction than during the dry season.
- Areas of existing landslides are more likely to move in future earthquakes than areas that have never experienced a landslide. If an earthquake occurs during the wet season, there will be more landslides than during the dry season.

The two following sections reflect our recommendations from this study and the limitations surrounding the datasets. Additional information regarding the application of these datasets within the Hazus model can be found in **Appendix A.**

5.1 Recommendations

Our analysis suggests a significant coseismic hazard in the study area. This amount of potential risk indicates a strong need for continuing coseismic hazard risk reduction. Therefore, we make the following recommendations.

Risk – Perform detailed risk assessments, engage stakeholders, and prioritize risk reduction and mitigation. Some of this work has been performed by Bauer and others (2018) and the Regional Disaster Preparedness Organization. Other recent efforts include the Portland Water Bureau Water System Seismic

Study (InfraTerra Inc. and Cascade GIS & Consulting LLC, 2016) and the Oregon Highways Seismic PLUS Report (Oregon Department of Transportation, 2014).

Awareness – Raising awareness of local hazards is crucial to understanding associated dangers and preparing for them. This report and maps in conjunction with earthquake risk assessments, such as that of Bauer and others (2018), can help emergency managers, planners, residents, and landowners in the study area become aware of the hazard and increase readiness for future events. Once the hazard is better understood, residents and landowners could work on risk reduction.

Planning – Planning is an effective method to work on risk reduction and can be initiated in a variety of ways using the data produced in this project. Leaders, residents, and landowners may consider both reducing risk to future development and mitigating risk for existing structures. These new hazard maps may also be used in long-term planning. The data can be included in assessments when discussing expansion of urban growth boundaries.

Emergency Response – These maps can be a valuable aid for emergency management activities such as development and refinement of emergency response plans, public outreach activities, selection of appropriate safe-haven sites, hazard response drills, and estimation of resource impacts for various earthquake hazard scenarios (Spangle Associates, 1998). In related applications, communities and others can use the landslide and liquefaction hazard maps to identify infrastructure that is likely to be damaged by major earthquakes. For example, by combining the hazard maps with transportation layers, potential road blockages can be identified and alternative corridors can be located. Similarly, the hazard maps can be combined with other information, such as the locations of hazardous waste facilities, to evaluate potential effects and to plan for emergency response.

Hazard Data Improvements – The methods used in this study reflect the current data inputs required by Hazus to model earthquake damages. However, these methods are several decades old and should be updated. As discussed in the Introduction section of this report, when one part of the method is updated, the rest of the related tables and equations must also be updated. Such updates would likely be labor intensive but may in some cases result in important improvements in the results. Some other improvements can include moving to a 3D geologic model so that the depth of groundwater and various surficial deposits can be included in the hazard analysis. This is important because at the surface there may be a highly liquefiable deposit, but if the deposit is only one meter thick and not saturated, liquefaction is unlikely to occur. For the coseismic landslide component, getting away from a grid type analysis would improve the model. When a landslide happens, it usually affects a large area simultaneously and with the same hazard and thus should not be analyzed grid cell by grid cell separately, especially with commonly smaller and smaller grid cells.

5.2 Limitations

Applicability of geohazard data – Methods used here and results are for Hazus-specific mapping. These maps are not intended to be used in place of site-specific mapping. The results are also intended to be used with the related Hazus tables and equations as discussed in the introduction of this report.

Limitations of source data – In this study, we used the best available landslide and geologic mapping available at a given location. Unfortunately, this results in highly variable quality of data across the study area. Some of these effects can be seen in the final maps as abrupt changes, for example in liquefaction and soil amplification along geologic unit boundaries. In the north-central portion of Washington County, there is an abrupt change along a north-south trending line that does not reflect a real geological change but instead is a product of different past mapping efforts (**Figure 12**).

Every effort has been made to ensure the accuracy of the GIS and tabular components of the source maps, but it is not feasible to verify all original input data. The GIS database is a "snapshot" view of current data and as such is inherently constrained by time. We also recognize that a single mapped geologic unit may include a variety of materials that may not all have the same landslide or liquefaction susceptibility rating and may not amplify ground motion in a uniform way. Further uncertainty is added in the interpretation of geologic units from past mapping. For example, an artificial fill in one location may have been constructed prior to the use of modern geotechnical engineering techniques and therefore may perform much worse than would a modern engineered, artificial fill. This type of detail is not commonly included in geologic mapping.

Very limited fieldwork – Very limited fieldwork was performed to create the final maps in this report. However, fieldwork was performed to create the source datasets used in this report including the lidar-derived digital elevation model and many of the source landslide inventories and the geologic maps. By definition, the soil amplification classified as type F requires further, site-specific examination. Because the Hazus model is unable to process class F units, Bauer and others (2018) chose to reclassify class F units as class E when running their analysis. This assumption may be valid for some type F soils but not for others.

When assessing landslide susceptibility based on topography, we encounter another limitation because the lidar-based digital elevation model (DEM) is a model of elevation; it does not distinguish elevation changes that may be due to manmade structures like retaining walls. It is not possible to conduct the extensive fieldwork required to locate all existing structures, determine the stability of each structure, and map each structure. Therefore, as a conservative approach, elevation changes not mapped as structures are assumed to be slopes; these must be examined on a site-specific basis. Prediction or estimation of displacement or runout of landslides is not included in maps produced following this method.

Dry or wet soil conditions – For landslides we created two maps using the Hazus method, one map for dry conditions and the other for wet conditions. These conditions are the end-members of a range of possibilities. The reality will likely be between these two and will fluctuate with seasonal moisture. The liquefaction maps do not have an assumed water table level as this information is incorporated into Hazus though a separate input dataset.

6.0 ACKNOWLEDGMENTS

The Regional Disaster Preparedness Organization (RDPO), Portland, Oregon, provided funding for this project through Urban Areas Security Initiative grant (UASI) 15-170 from U.S. Department of Homeland Security (Funding Opportunity [NOFO] #DHS-15-GPD-067-000-01; Federal Award Identification Number [FAIN] EMW-2015-SS-0004-S01). The Oregon Office of Emergency Management administered the grant on behalf of RDPO. We would like to thank DOGAMI staff who helped with this project through technical and general assistance and review, especially Ian Madin, Yumei Wang, and Deb Schueller. Our sincere thanks to Ray Wells and the USGS for sharing some geologic data used in this study.

7.0 REFERENCES

Bauer, J. M., Burns, W. J., and Madin, I. P., 2018, Earthquake regional impact analysis for Clackamas, Multnomah, and Washington Counties, Oregon: Oregon Department of Geology and Mineral Industries, Open-File Report O-18-02. https://www.oregongeology.org/pubs/ofr/p-O-18-02.htm

Buildings Seismic Safety Council, 1997, NEHRP recommended provisions for seismic regulations for new buildings and other structures: Washington, D.C., report prepared for Federal Emergency Management Administration. http://www.ce.memphis.edu/7137/PDFs/fema302a.pdf

Burns, W. J., and Madin, I. P., 2009, Protocol for inventory mapping of landslide deposits from light detection and ranging (lidar) imagery: Oregon Department of Geology and Mineral Industries, Special Paper 42. https://www.oregongeology.org/pubs/sp/p-SP-42.htm

Burns W. J., and Watzig, R. J., 2017, Statewide Landslide Information Database for Oregon [SLIDO], release 3.4: Oregon Department of Geology and Mineral Industries, Digital Data Series. https://www.oregongeology.org/slido/

Burns, W. J., Hofmeister, R. J., and Wang, Y., 2008, Geologic hazards, earthquake and landslide hazard maps, and future earthquake damage estimates for six counties in the Mid/Southern Willamette Valley including Yamhill, Marion, Polk, Benton, Linn, and Lane Counties, and the City of Albany, Oregon: Oregon Department of Geology and Mineral Industries, Interpretive Map IMS-24. https://www.oregongeology.org/pubs/ims/p-ims-024.htm

Burns, W. J., Hughes, K. B., Olson, K. V., McClaughry, J. D., Mickelson, K. A., Coe, D. E., English, J. T., Roberts, J. T., Lyles Smith, R. R., and Madin, I. P., 2011, Multi-hazard and risk study for the Mount Hood region, Multnomah, Clackamas, and Hood River Counties, Oregon: Oregon Department of Geology and Mineral Industries, Open-File Report O-11-16. https://www.oregongeology.org/pubs/ofr/p-O-11-16.htm

Burns, W. J., Mickelson, K. A., Jones, C. B., Pickner, S. G., Hughes, K. L., and Sleeter, R., 2013, Landslide hazard and risk study of northwestern Clackamas County, Oregon: Oregon Department of Geology and Mineral Industries, Open-File Report O-13-08. https://www.oregongeology.org/pubs/ofr/p-O-13-08.htm

Burns, W. J., Mickelson, K. A., Jones, C. B., Tilman, M. A., and Coe, D.E., 2015, Surficial and bedrock engineering geology, landslide inventory and susceptibility, and surface hydrography of the Bull Run Watershed, Clackamas and Multnomah Counties, Oregon: Oregon Department of Geology and Mineral Industries, Special Paper 46. https://www.oregongeology.org/pubs/sp/p-SP-46.htm

Federal Emergency Management Agency (FEMA), 2003, Hazus-MH, FEMA's tool for estimating potential losses from natural disasters, Earthquake Technical Manual: Washington, D. C., National Institute of Building Sciences. (Also available on CD-ROM from FEMA: https://www.fema.gov/media-library/assets/documents/24609)

Federal Emergency Management Agency (FEMA), 2011, Hazus®-MH 2.1 Technical manual, Earthquake Model: Washington, D.C., 718 p. https://www.fema.gov/media-library/assets/documents/24609

Geotechnical Extreme Events Reconnaissance Association (GEER), 2011, Geotechnical engineering reconnaissance of the 2011 Christchurch, New Zealand earthquake, ver. 1.0, August 15, 2011, Report No. GEER-027. doi:10.18118/G68G65

Geotechnical Extreme Events Reconnaissance Association (GEER), 2017, Geotechnical engineering reconnaissance of the 19 September 2017 Mw 7.1 Puebla-Mexico City earthquake, ver. 2.0, February, 16, 2017, Report No. GEER-055A. doi:10.18118/G6JD46

Hofmeister, R. J., Hasenberg, C. S., Madin, I. P., and Wang, Y., 2003a, Relative earthquake and landslide hazards in Clackamas County: Oregon: Oregon Department of Geology and Mineral Industries, Open-File Report O-03-09. https://www.oregongeology.org/pubs/ofr/O-03-09.pdf

Hofmeister, R. J., Hasenberg, C. S., Madin, I. P., and Wang, Y., 2003b, Earthquake and landslide hazard maps, and future earthquake damage estimates, for Clackamas County, Oregon: Oregon Department of Geology and Mineral Industries, Open-File Report O-03-10. https://www.oregongeology.org/pubs/ofr/O-03-10.zip

InfraTerra Inc. and Cascade GIS & Consulting LLC, 2016, Portland Water Bureau seismic study 2016.

Kramer, S. L., 1996, Geotechnical earthquake engineering: Prentice Hall, New Jersey, 653 p.

Ma, L., Madin, I. P., Duplantis, S., and Williams, K. J., 2012, Lidar-based surficial geologic map and database of the greater Portland, Oregon, area, Clackamas, Columbia, Marion, Multnomah, Washington, and Yamhill Counties, Oregon, and Clark County, Washington: Oregon Department of Geology and Mineral Industries Open-File Report O-12-02, 30 p. https://www.oregongeology.org/pubs/ofr/p-O-12-02.htm

Mabey, M. A., Madin, I. P., Drescher, D. E., Uba, O. G., and Bosworth, M., 1993a, Relative earthquake hazard map of the Portland, Oregon 7 1/2-minute quadrangle: Oregon Department of Geology and Mineral Industries, Open-File Report O-93-14. https://www.oregongeology.org/pubs/ofr/O-93-14.pdf

Mabey, M. A., Madin, I. P., Youd, T.L., and Jones, C.F., 1993b, Earthquake hazard maps of the Portland quadrangle, Multnomah and Washington Counties, Oregon, and Clark County, Washington: Oregon Department of Geology and Mineral Industries, Geologic Map Series, GMS-79. https://www.oregongeology.org/pubs/gms/GMS-079.pdf

Mabey, M. A., Madin, I. P., and Meier, D. B., 1995a, Relative earthquake hazard map of the Beaverton quadrangle, Washington County, Oregon: Oregon Department of Geology and Mineral Industries, Geologic Map Series, GMS-90. https://www.oregongeology.org/pubs/gms/GMS-090.zip

Mabey, M. A., Madin, I. P., and Meier, D. B., 1995b, Relative earthquake hazard map of the Lake Oswego quadrangle, Clackamas, Multnomah, and Washington Counties, Oregon: Oregon Department of Geology and Mineral Industries, Geologic Map Series, GMS-91. https://www.oregongeology.org/pubs/gms/GMS-091.zip

Mabey, M. A., Madin, I. P., and Meier, D. B., 1995c, Relative earthquake hazard map of the Gladstone quadrangle, Clackamas and Multnomah Counties, Oregon: Oregon Department of Geology and Mineral Industries, Geologic Map Series, GMS-92. https://www.oregongeology.org/pubs/gms/GMS-092.pdf

Mabey, M. A., Meier, D. B., and Palmer, S. P., 1995d, Relative earthquake hazard map of the Mount Tabor quadrangle, Multnomah County, Oregon, and Clark County, Washington: Oregon Department of Geology and Mineral Industries, Geologic Map Series, GMS-89. https://www.oregongeology.org/pubs/gms/GMS-089.pdf

Mabey, M. A., Madin, I. P., Black, G. L., and Meier, D. B., 1996, Relative earthquake hazard map of the Linnton quadrangle, Multnomah and Washington Counties, Oregon: Oregon Department of Geology and Mineral Industries, Geologic Map Series, GMS-104. https://www.oregongeology.org/pubs/gms/GMS-104.zip

Mabey, M. A., Black, G. L., Madin, I. P., Meier., D. B., Youd, T. L., Jones, C. F., and Rice, J. B., 1997, Relative earthquake hazard map of the Portland metro region, Clackamas, Multnomah, and Washington Counties, Oregon: Oregon Department of Geology and Mineral Industries, Interpretive Map Series, IMS-1. https://www.oregongeology.org/pubs/ims/IMS-001.zip

Madin, I. P., 1990, Earthquake-hazard geology maps of the Portland metropolitan area, Oregon: Text and map explanation. Oregon Department of Geology and Mineral Industries, Open-File Report O-90-02. https://www.oregongeology.org/pubs/ofr/O-90-02.pdf

Madin, I.P., and Burns, W. J., 2013, Ground motion, ground deformation, tsunami inundation, coseismic subsidence, and damage potential maps for the 2013 Oregon Resilience Plan for Cascadia Subduction Zone Earthquakes: Oregon Department of Geology and Mineral Industries, Open-File Report O-13-06. https://www.oregongeology.org/pubs/ofr/p-O-13-06.htm

Madin, I. P., and Wang, Z., 1999a, Relative earthquake hazard maps for selected urban areas in western Oregon: Dallas, Hood River, McMinnville-Dayton-Lafayette, Monmouth-Independence, Newburg-Dundee, Sandy, Sheridan-Willamina, St. Helens-Columbia City-Scappoose: Oregon Department of Geology and Mineral Industries, Interpretive Map Series, IMS-7. https://www.oregongeology.org/pubs/ims/IMS-007.zip

Madin, I. P., and Wang, Z., 1999b, Relative earthquake hazard maps for selected urban areas in western Oregon: Canby-Barlow-Aurora, Lebanon, Silverton-Mount Angel, Stayton-Sublimity-Aumsville, Sweet Home, Woodburn-Hubbard: Oregon Department of Geology and Mineral Industries, Interpretive Map Series, IMS-8. https://www.oregongeology.org/pubs/ims/IMS-008.zip

Mickelson, K. A., and Burns, W. J., 2012, Landslide hazard and risk study of the U.S. Highway 30 Corridor, Clatsop and Columbia Counties, Oregon: Oregon Department of Geology and Mineral Industries, Open-File Report O-12-06. https://www.oregongeology.org/pubs/ofr/p-O-12-06.htm

Natural Resources Conservation Service, 2018, Online soil survey geodatabase and Access® tables: U.S. Department of Agriculture, accessed July 10, 2018. https://websoilsurvey.nrcs.usda.gov/app/WebSoilSurvey.aspx for Columbia County: https://websoilsurvey.sc.egov.usda.gov/DSD/Download/Cache/SSA/wss_SSA_OR009_soildb_OR_2003_[2019-09-10].zip; Multnomah County: https://websoilsurvey.sc.egov.usda.gov/DSD/Download/Cache/SSA/wss_SSA_OR051_soildb_OR_2003_[2019-09-10].zip; Washington County: https://websoilsurvey.sc.egov.usda.gov/DSD/Download/Cache/SSA/wss_SSA_OR067_soildb_OR_2003_[2019-09-10].zip

Oregon Department of Transportation (ODOT), 2014. Oregon Highways Seismic PLUS Report, Bridge and Geo-Environmental Sections, https://www.oregon.gov/ODOT/Bridge/Docs_Seismic/Seismic-Plus-Report_2014.pdf

Roe, W. P., and Madin, I. P., 2013, 3D geology and shear-wave velocity models of the Portland, Oregon, metropolitan area, Oregon Department of Geology and Mineral Industries, Open-File Report O-13-12. https://www.oregongeology.org/pubs/ofr/p-O-13-12.htm

Smith, R. L., and Roe, W. P., compilers, 2015, Oregon geologic data compilation (OGDC), release 6 (statewide): Oregon Department of Geology and Mineral Industries, Digital Data Series. https://www.oregongeology.org/pubs/dds/p-OGDC-6.htm

Spangle Associates, 1998, Using earthquake hazard maps: A guide for local governments in the Portland Metropolitan Region: Oregon Department of Geology and Mineral Industries, Open-File Report O-98-4, 45 p. https://www.oregongeology.org/pubs/ofr/O-98-04.pdf

Stone, W. C., Yokel, F. Y., Celebi, M., Hanks, T., and Leyendecker, E. V., 1987, Engineering aspects of the September 19, 1985 Mexico earthquake, NIST Building Science Series 165, https://nvlpubs.nist.gov/nistpubs/Legacy/BSS/nbsbuildingscience165.pdf

U.S. Census Bureau, 2019, Quick Facts: U.S. Census Bureau database. Accessed May 1, 2019. https://www.census.gov/quickfacts/fact/table/US/PST045218

van Rijsingen, E., 2017, How Rome and its geology are strongly connected: European Geosciences Union (EGU), Tectonics and Structural Geology (TS) Division blog, December 3, 2017. https://blogs.egu.eu/divisions/ts/2017/12/03/how-rome-and-its-geology-are-strongly-connected/

Wang, Y., Weldon, R., and Fletcher, D., 1998, Creating a UBC soil map for Oregon: Oregon Geology, v. 60, no 4. p. 74-78. https://www.oregongeology.org/pubs/og/OGv60n04.pdf

Wieczorek, G. F., Wilson, R. C., and Harp, E. L., 1985, Map of slope stability during earthquakes in San Mateo County, California: U.S. Geological Survey, Miscellaneous Investigations Map I-1257-E. https://pubs.usgs.gov/imap/1257e/report.pdf

Wilson, R. C., and Keefer, D. K., 1985, Predicting areal limits of earthquake-induced landsliding, *in* Ziony, J. L., ed., Evaluating earthquake hazards in the Los Angeles region; an earth-science perspective: U.S. Geological Survey Professional Paper 1360, p. 316–345.

Youd, T. L., and Perkins, D. M., 1978, Mapping of liquefaction induced ground failure potential: Journal of the Geotechnical Engineering Division, American Society of Civil Engineers, v. 104, no. 4, p. 433–446.

APPENDIX A. APPLICATIONS OF MAPS WITHIN HAZUS

The four maps produced by this study are intermediary datasets within the Hazus earthquake modeling and loss estimation process (FEMA, 2011). This section of this report was added to assist users in understanding what the susceptibility maps mean and how Hazus software incorporates coseismic hazard data into its earthquake modeling.

The soil amplification class, liquefaction susceptibility, and landslide susceptibility maps are based on interpretations of mapped geologic units and must be combined with additional information about the specific characteristics of the earthquake and groundwater levels to understand the likelihood of coseismic hazard occurring in a given area. Key datasets, such as depth of groundwater or amplitude and duration of ground shaking, are included separately within the Hazus model. To provide an example of the way in which Hazus combines the susceptibility maps with other datasets to produce liquefaction probability maps and ground deformation models, we summarize information found in the Hazus Earthquake Technical Manual (FEMA, 2011, Section 4). We recommend that users who want to learn more about the applications of each of the coseismic hazard susceptibility maps in Hazus consult the FEMA manual.

As an example, the liquefaction susceptibility maps produced in this study are only one piece of a larger method used by Hazus to determine the likelihood of a given location experiencing liquefaction during an earthquake. As shown in **Figure 15**, liquefaction susceptibility classifications (shown in the green box) are used to determine the conditional liquefaction probability for a given ground shaking amplitude (shown in pale blue) and the proportion of map unit susceptible to liquefaction (shown in orange) for each map unit. These two values are combined with information regarding the magnitude of the seismic event (shown in pale yellow) and depth to groundwater (shown in pink) to calculate the liquefaction probability using the following equation (FEMA, 2011, equation 4-20):

$$P[\text{Liquefaction}_{SC}] = \frac{P[\text{Liquefaction}_{SC}|PGA = a]}{K_M \cdot K_w} \cdot P_{ml}$$

where

$P[\text{Liquefaction}_{SC}]$ is the probability of liquefaction for a given susceptibility category

$P[\text{Liquefaction}_{SC}|PGA = a]$ is the conditional liquefaction probability for a given susceptibly category at a specified level of peak ground acceleration

K_M is the moment magnitude (M) correction factor

K_w is the groundwater correction factor

P_{ml} is the proportion of map unit susceptible to liquefaction

This equation is summarized in the light purple oval in **Figure 15**. Within Hazus this final liquefaction probability map (shown in bright yellow) is further combined with several additional datasets including landslide probability, ground motion, and ground amplification to model permanent ground deformation (shown in bright blue).

Figure 15. Summary of application of liquefaction susceptibility maps within Hazus (FEMA, 2011).

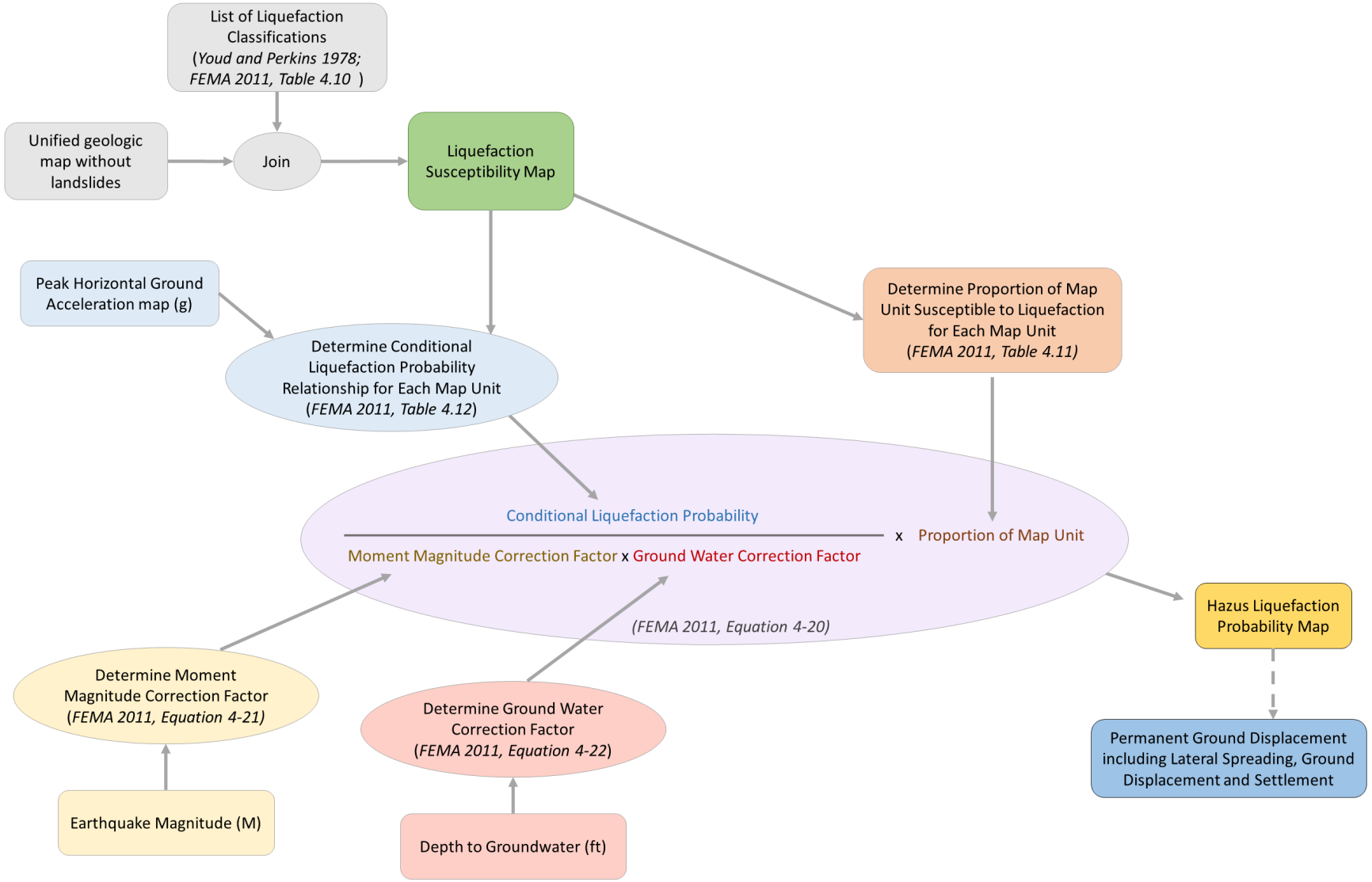

With this method, we can estimate the probability of liquefaction for an area of uncompacted, artificial fill liquefying during a magnitude 9.0 earthquake, with a peak horizontal ground acceleration of 0.15 g and groundwater depth of 3 ft. Under these conditions, the soil type is very highly susceptible to liquefaction, the conditional probability would be 0.5435, 25% of the unit would be likely to liquefy, the moment magnitude correction factor would be 0.8749, and the groundwater correction factor would be 0.9960. As a result, the combined liquefaction probability for this map unit would be 15.6%.

Like the liquefaction susceptibility dataset, landslide susceptibility and soil amplification class datasets are combined with additional information about the specific characteristics of the earthquake when these datasets are used in Hazus before they directly inform the ground motion, amplification, displacement, and finally estimations of damage and loss.

Many other methods exist to create coseismic landslide and liquefaction hazard datasets and result in different types of output maps. For example, a liquefaction hazard map could be made with a series of assumptions or additional datasets such as the magnitude of the earthquake for which the map applies or the depth of the groundwater throughout the map extent. The output map following a method like this could have hazard classes just like the Hazus-based susceptibility (low, moderate, high, etc.) but have a different meaning. For example, "high" might mean there is greater than one meter of settlement predicted with a ground motion from a magnitude 9.0 earthquake with a certain ground water level on one map and mean 20% of that map unit might have liquefaction if several factor thresholds are reached in a specific earthquake scenario on another map.

Because of all of these specifics, care should be taken when using the maps created in this report and when comparing these maps to other maps. If any of the coseismic classifications are produced following methods other than those described in Hazus, not only will the susceptibility rating mean something different, but the data will not be compatible with the Hazus earthquake modeling process. More information regarding the Hazus-compatible method used in this study can be found in FEMA's Hazus Earthquake Technical Manual, Section 4 (2011).

APPENDIX B. GEOLOGIC UNIT CLASSIFICATION

Table B-1. Soil amplification classification for geologic units from Ma and others (2012). NEHRP is National Earthquake Hazard Reduction Program.

General Description	Map Unit Name and Abbreviation	NEHRP Class
Aeolian Deposits	Aeolian deposits (Qe), Primary loess (Ql)	D
Aeolian Deposits	Floodplain dune deposits (Hfd)	E
Alluvium	Estacada terrace of the Clackamas River (Htce), Subterraces of the Estacada Terrace of the Clackamas River (Htcx), Middle Clackamas terraces (Qtcm), Subterraces of the middle terrace of the Clackamas River (Qtcmx), Upper Clackamas River terrace (Qtcu), Clackamas River terraces undifferentiated (Qtcx)	D
Alluvium	Alluvium of the Clackamas River (Hacl), Alluvium of the Columbia River (Haco), Alluvium of lowland streams (Hal), Alluvium of the Molalla-Pudding Rivers (Ham), Alluvium of the Sandy River (Has), Alluvium of the Tualatin River (Hat), Alluvium of the Willamette River (Haw), Sandy River volcanogenic delta (Hsd), Terraces of Abernathy Creek (Hta), Terrace deposits of the Willamette River (Htw), Alluvium of minor streams (Qal), Pond Deposits (Qp), Terrace deposits of the Sandy River (Qtsu), Terrace deposits of the Tualatin Mountains (Qttm)	E
Artificial Fill	Artificial fill (Aaf)	F
Missoula Flood Deposits	Missoula flood deposits, coarse-grained facies (Qmc)	C
Missoula Flood Deposits	Missoula flood deposits, channel facies (Qmch), Missoula flood deposits, fine-grained (Qmf), Missoula floods silt colluvium (Qmf-c)	D
Sedimentary Bedrock	Hillsboro Formation (QTh), Springwater Formation (QTs), Rhododendron Formation (Tr), Scappoose Formation (Ts), Troutdale Formation, conglomerate (Ttg), Troutdale Formation, mudstone facies (Ttm), Troutdale Formation, sandstone (Tts)	C
Sedimentary Bedrock with Loess	Hillsboro Formation and loess (QTh-l), Springwater Formation and loess (QTs-l), Troutdale Formation, conglomerate (Ttg-l)	D
Volcanic Bedrock	Basaltic andesite of Anderson (Qba), Basaltic andesite of Barnes Road (Qbab), Basaltic andesite of Broughton Bluff (Qbbb), Basalt of Carver (Qbca), Basalt of Douglass Ridge (Qbd), Basaltic andesite of Hunsinger (Qbh), Basaltic andesite of Hardscrabble (Qbhs), Basalt of Jenne (Qbj), Basalt of Kelly Butte (Qbkb), Basalt of Mount Talbert (Qbm), Basalt of Mount Tabor (Qbmt), Basaltic andesite of Outlook (Qbo), Basalt of Powell Butte (Qbp), Basalt of Borges Road (Qbr), Basaltic andesite of Rocky Butte (Qbrb), Basalt of Mount Scott (Qbs), Basalt of Mount Sylvania (Qbsy), Basalt of Winston Road (Qbw), Undivided basalt and basaltic andesite (QTb), Basalt of Tong Road (QTbt), Basalt of Zion Hill (QTbz), Volcanic sandstone and conglomerate (Qvca), Outlook tephra (Qvo), Tephra of basalt of Rodlun Road (Qvrr), Basaltic andesite of Beaver Creek (Tbb), Basalt of Canemah (Tbc), Basalt of Cooks Butte (Tbcb), Basaltic andesite of Fallsview (Tbf), Basaltic andesite of Highland Butte (Tbh), Basaltic andesite of Root Creek (Tbr), Undifferentiated Columbia River Basalt Group (Tcr), Ortley Member (Tgo), Undifferentiated Grande Ronde Basalt (Tgr), Sentinel Bluffs Member (Tgsb), Basalt of Umtanum (Tgu), Winter Water Member (Tgww), Canemah tephra (Tvc), Fallsview tephra (Tvf), Root Creek tephra (Tvr), Basalt of Gingko (Twfg), Basalt of Sentinel Gap (Twfsg), Basalt of Sand Hollow (Twfsh), Basalt of Waverly Heights and associated undifferentiated sedimentary rocks (Twh), N2 and R2 Flows Undivided (Tgru)	C
Volcanic Bedrock with Loess	Basaltic andesite of Elk Point and loess (Qbae-l), Basalt of Kaiser Road and loess (Qbk-l), Basalt of Rodlun Road and loess (Qbrr-l), Basalt of Mount Sylvania and loess (Qbsy-l), Basaltic andesite of Bonny Slope and loess (QTbb-l), Tephra of Jenne and loess (Qvj-l), Undifferentiated Columbia River Basalt Group (Tcr-l), Ortley Member (Tgo-l), Sentinel Bluffs Member and loess (Tgsb-l), Basalt of Wapshilla Ridge and loess (Tgwr-l), Winter Water Member and loess (Tgww-l), Basalt of Gingko (Twfg-l), Basalt of Sand Hollow (Twfsh-l), Basalt of Waverly Heights and loess (Twh-l)	D

Table B-2. Soil amplification classification for geologic units from R. Wells and others (unpub. data, 2017). NEHRP is National Earthquake Hazard Reduction Program.

General Description	Map Unit Name and Abbreviation	NEHRP Class
Aeolian Deposits	Eolian deposits (Qe), Loess (Ql)	D
Alluvium	Deposits of Ape Canyon and Older (Qsa)	C
Alluvium	Gravel of Coast Range provenance (Qgcr), Oldest, pre-Missoula deposits (Qh1), Older gravel of Cascade arc origin (QTca), Terrace deposits (Qtd), Older terrace deposits (Qto), Older Gravel of Columbia River Origin (QTcr)	D
Alluvium	Alluvium (Qa), Alluvial fan deposits (Qaf), Older, post-Missoula deposits (Qh2), Youngest deposits (Qh3), Lacustrine deposits (Qla), Younger terrace deposits (Qty)	E
Artificial fill	Artificial fill (af)	F
Colluvium	Basaltic colluvium (Qcb), Talus (Qt)	F
Missoula Flood Deposits	Coarse Grained Missoula Flood Deposits (Qfc)	C
Missoula Flood Deposits	Missoula Flood deposits (Qf)	D
Sedimentary Bedrock	Cowlitz Formation (Tc), Cowlitz Formation: C&W sandstone member (Tc1), Cowlitz Formation: Upper mudstone member (Tc2), Hamlet Formation (Th), Hamlet Formation: Roy Creek Member (Thr), Hamlet Formation: Sunset Highway Member (Ths), Hamlet Formation: Sweet Home Creek Member (Thsw), Keasey Formation (Tk), Keasey Formation: Jewell member (Tkj), Keasey Formation: Middle member (Tkm), Keasey Formation, Upper member (Tku), Mist Formation: Gus Creek conglomerate (Tmgc), Mist Formation: Windy Ridge member (Tmwr), Pittsburg Bluff Formation: East Fork Member (Tpe), Pittsburg Bluff Formation: Pebble Creek Member (Tpp), Pittsburg Bluff Formation: Stimson Mill Member (Tpsm), Pittsburg Bluff Formation: Tuff bed (Tpst), Scappoose Formation (Ts), Scappoose Formation: Divide Member (Tsd), Scappoose Formation: Dairy Creek Member (Tsdc), Scappoose Formation: Sandy River Mudstone (Tsm), Scappoose Formation: Oak Ranch Creek Member (Tsoc), Siletz River Volcanics: Silty interbeds (Tsrf), Scappoose Formation: Ribbon Ridge member (Tsrs), Troutdale Formation: Hyaloclastite sandstone (Tth), Yamhill Formation (Ty), Pittsburg Bluff Formation (Tpb), Sager Creek Formation (Tsc)	C
Volcanic Bedrock	Boring Volcanics (2.2-2.7 Ma) (QTb1), Boring Volcanics (1.4-1.7 Ma) (QTb3), Grande Ronde Basalt: Armstrong Canyon member (Tgac), Grande Ronde Basalt: Buttermilk Canyon member (Tgbc), Grande Ronde Basalt: Downey Gulch Member (Tgdg), Grande Ronde Basalt: Grouse Creek Member (Tggc), Grande Ronde Basalt: N2 flows (TgN2), Grande Ronde Basalt: Ortley Member (Tgo), Grande Ronde Basalt: N2 and R2 flows (Tgru), Grande Ronde Basalt: Sentinel Bluff Member (Tgsb), Grande Ronde Basalt: Umtanum Member (Tgu), Grande Ronde Basalt: Wapshilla Ridge Member (Tgwr), Grande Ronde Basalt: Winter Water Member (Tgww), Basalt of the High Cascades (Thb), Intrusive Grande Ronde Basalt (Tig), Intrusive rocks of the Coast Range (Tis), Goble Volcanics (Togv), Siletz River Volcanics: Subaerial rocks (Tsra), Siletz River Volcanics: Submarine flows and breccias (Tsrm), Tillamook Volcanics (Ttv), Tillamook Volcanics: Subaerial flows (Ttva), Submarine flows and breccias (Ttvm), Frenchman Springs Member (Twf), Basalt of Gingko of Mackin (1961) (Twfg), Basalt of Sand Hollow of Mackin (1961) (Twfh), Basalt of Sentinel Gap of Mackin (1961) (Twfs), Basalt of Rosalia of Beeson and others (1989) (Twpr), Andesite of the Western Cascades (Tyva), Scaponia Tuff (Tps), Older Intrusions of the Western Cascade Range (Tio), Clastic Rocks Associated with Grande Ronde Basalt (Tgc), Grouse Creek Member (Tgr2)	C
Water	Water (water)	E

Table B-3. Soil amplification classification for geologic units from OGDC-6 (Smith and Roe, 2015). NEHRP is National Earthquake Hazard Reduction Program.

General Description	Map Unit Name and Abbreviation	NEHRP Class
Aeolian	Primary Loess (Ql)	D
Alluvium	Sand and gravel that predates Missoula Floods (Qg2), Outwash (Qo), Older alluvial deposits (Qoal), Older alluvial deposits (Qoal1), Terrace gravels (Qtg), Weathered terrace gravel (QTg)	D
Alluvium	Alluvial deposits (Qal), Alluvium (Qal), Quaternary alluvium (Qal), Floodplain deposits of the Willamette River and major tributaries (Qalc), Alluvium of smaller streams (Qalf), Alluvium, undifferentiated (Qau), Sand and gravel that postdates Missoula Floods (Qg1), High terrace gravels (Qt), Alluvium (Qa1), Terrace Deposits (Qt), Pond Deposits (Qp), Lacustrine Deposits (Qlc), Alluvium (Qal1), Alluvium (Qa),	E
Artificial Fill	Artificial fill (af)	F
Colluvium	Glacial deposits (Qg), Glacial till (Qg), Till of Evans Creek age (Qget), Glacial moraine and outwash deposits (Qgl), Till of neoglacial age (Qgnt), Glacial drift (Qt), Younger till (Qyt), Pre-CRB Conglomerate (Toc)	C
Colluvium	Pyroclastic flow and debris-flow deposits (Qhc), Pyroclastic-flow and debris-flow deposits (Qhoc), Pyroclastic flow and debris-flow deposits (Qhpc), Pyroclastic flow and debris-flow deposits (Qhtc)	D
Colluvium	Flow and Fan Deposits (Qf)	
Colluvium	Talus (Qt), Talus deposits (Qt), Talus (Qta)	F
Missoula Flood Deposits	Coarse Missoula Flood deposits (Qfc), Missoula (Bretz) Flood deposits (Qff), Cataclysmic Flood Deposits: Gravel Facies (Qfg), Cataclysmic Flood Deposits: Silt and Sand Facies (Qfs), Missoula Flood Deposits (Qmf)	C
Missoula Flood Deposits	Main body of fine-grained Missoula Flood deposits (Qff2)	D
Mixed Bedrock	Tuffaceous sedimentary rocks, basalt flows, and tuffs, undivided (Tu), Tertiary and Quaternary volcanic and sedimentary rocks and deposits, undivided (Tv), Colluvial and alluvial slope deposits (Qca), Fluvial and lacustrine(?) sedimentary deposits (Tfl)	C
Mixed Colluvium and Alluvium	Glacio-fluvial deposits (Qgf), Conglomerate (QTc)	D
Sedimentary Bedrock	Quaternary sediment and sedimentary rocks, undivided (Qs), Springwater Formation (QTs), Troutdale Formation (QTt), Troutdale Formation, Upper Member (QTtu), Basaltic sandstone at Roy Creek (Tbs), Continental sedimentary rocks (Tcs), Rhododendron Formation (Tmpr), Fossiliferous sandstones and tuffaceous claystones (Tom1), tuffaceous arkose (Tom2), Coal-bearing conglomerates and claystones (Tom3), Older sedimentary rocks (Tos), Consolidated fluvial deposits (Tpf), Troutdale Formation (Tpt), Rhododendron Formation (Tr), Rhododendron Formation (Trh), Sedimentary rocks (Ts), Tertiary sedimentary rocks (Ts1), Tertiary sedimentary rocks (Ts3), Tertiary sedimentary rocks (Ts4), Sardine Formation, tuffaceous nonmarine sedimentary rocks (Tsat), Scotts Mills Formation (Tsm), Scotts Mills Formation, undifferentiated (Tsm), Scotts Mills Formation, Abiqua Member (Tsma), Scotts Mills Formation, Crooked Finger Member (Tsmc), Troutdale Formation (Tt), Troutdale Formation, Lower Member (Ttl), Troutdale Formation mudstone and siltstone (Ttm), Troutdale Formation volcaniclastic sandstone (Tts), Yamhill Formation (Ty), Younger sedimentary rocks (Tys), Yamhill Formation, lower tuff unit (Tyt), Scappoose Formation (Ts1), Pittsburg Bluff Formation: Connors Creek Member (Tpbcc), Pittsburg Bluff Formation (Tpb), Scappoose Formation: interbeds, shelf sandstone (Ts2), Keasey Formation (Tk), Sandy River Mudstone (Tsr), Troutdale Formation (Ttf), Astoria Formation (TA), Astoria Formation (TA1), Pittsburg Bluff Formation: Laminated Member (Tpl), Pittsburg Bluff Formation: Siltstone Member (Tps), Scappoose Formation: Shelf Sandstone Unit (Ts), Cowlitz Formation (Tc), Scappoose Formation: Shelf Sandstone (Tso), Troutdale Formation: Coarse Grained (QTtd), Cowlitz Formation: Clark and Wilson Sandstone Member (Tccw), Cowlitz Formation: Upper Mudstone Member (Tcum), Hamlet Formation: Sweet Home Creek Mudstone Member (Thsw), Undifferentiated Oligocene and Miocene Units (Tom), Hamlet Formation: Roy Creek Conglomerate Member (Thr), Hamlet Formation: Sunset Highway Sandstone Member (Thsh), Troutdale Formation (Ttd), Keasey Formation: Vesper Church Member (Tkv), Oligocene Sediment: Shelf Sandstone (Tos), Troutdale Formation (Tt)	C
Sedimentary Bedrock	Sandstone of Trask River (Trsk)	D
Volcanic Bedrock	Andesite of Cabin Creek (Qac), Andesite west of Clear Lake (Qacl), Andesite of Enola Hill (Qae), Andesite of Hiyu Mountains (Qah), Andesite of Horseshoe Ridge (Qahr), Andesite of Skyline Road (Qas), Andesite of Wapinitia Pass (Qaw), High Cascade lavas, basalt and basaltic andesite (Qb), Basaltic andesite and basalt (Qba), Basalt of Crutcher Bench (Qbc), Basaltic andesite of Devil Canyon (Qbdc), Hornblende-bearing basaltic andesite (Qbh), Basaltic andesite of Sisi Butte (Qbs), Dacite of Frog Lake Buttes (Qdf), Andesite and dacite lava (Qha), Lava (Qhol), Lava (Qhpl), Olivine basalt (Qob), Older basaltic andesite (Qoba), Andesite of Tom Dick and Harry Mountain (QTat), Basalt (QTb), Basalt and basaltic andesite (QTba), Basalt andesite (QTba), Basaltic andesite and basalt (QTba), Basaltic andesite of Mirror Lake and Eureka Peak (QTbme), Younger basaltic andesite (Qyba), Columbia River Basalt Group and related flows (Tc), Columbia River Basalt Group, undivided (Tc), Grande Ronde Basalt, normal polarity unit 2 (Tcgn2), Grande Ronde Basalt, reversed polarity unit 2 (Tcgr2), Columbia River Basalt group, lower part (Tcl), Columbia River Basalt Group (Tcr), Wanapum Basalt, Frenchman Springs member (Tcwf), Wanapum Basalt, Priest Rapids member (Tcwpr), Eagle Creek Formation (Tec), Columbia River Basalt Group, Wanapum Basalt, Frenchman Springs Member (Tf), Basalt of Silver Falls (Tfsf), Basalt of Sand Hollow (Tfsh), Grande Ronde Basalt, high Mg chemical type (Tgh), Columbia River Basalt Group, Grande Ronde Basalt, N1 Low MgO Chemical Type (Tgn1l), Grande Ronde Basalt, upper flows, normal magnetic polarity (Tgn2), N2 High MgO Chemical Type (Tgn2h), Columbia River Basalt Group, Grande Ronde Basalt, N2 Low MgO Chemical Type (Tgn2l), Columbia River Basalt Group, Grande Ronde Basalt, Winter Water Flow (Tgn2w), Ortley and Umtanum members (Tgou), Grande Ronde Basalt (Tgr), Grande Ronde Basalt, undivided (Tgr), Columbia River Basalt Group, Grande Ronde Basalt, R2 Low MgO Chemical Type (Tgr2l), Winter Water member (Tgww), Intrusive basalt (Tib), Columbia River Basalt Group, Pomona Member (Tp), Columbia River Basalt Group, Priest Rapids Member (Tpr), Wanapum Basalt, Frenchman Springs Member (Twf), Wanapum Basalt (Twp), Wanapum Basalt, Priest Rapids Member (Twp), Yakima Basalt Subgroup of the Columbia River Basalt Group (Tyb), Yakima Basalt Subgroup Of The Columbia River Basalt Group (Tyb), Columbia River Basalt Group, Frenchman Springs Member (Tyfs), Grande Ronde Basalt, Lower Low MgO Geochemical Type (Tygr0), Grande Ronde Basalt, Middle Low MgO Geochemical Type (Tygr1), Grande Ronde Basalt, Upper Low MgO Geochemical Type (Tygr2), Grande Ronde Basalt, High MgO Geochemical Type (Tygr3), Prineville Geochemical Type (Typv), Grouse Creek Member (Tgr2), Grays River Volcanics (Tgrv), Wapshilla Ridge Member Basalt (Tgr1), Winter Water Member Basalt (Tgr3), Grande Ronde Basalt (Tgru), Grande Ronde Basalt Member: Winter Water (Tgww), Grande Ronde Basalts Member: Ortley (Tgo), Columbia River Basalt (Tcr), Grande Ronde Basalt: Low MgO (Tgl), Grande Ronde Basalt: High MgO (Tgh), Grande Ronde Basalt (Tgr), Grays River Volcanics Basalt (Tgv), Columbia River Basalt Group (Tco), Columbia River Basalt Group (Tcrb)	B
Volcanic Bedrock	Dike (Dike), Dikes (dike), Dike (Dike1), Fault breccia (breccia), Younger basalt and basaltic andesite (Qb), Quaternary basaltic and andesitic rocks (Qb4), Quaternary basaltic and andesitic rocks (Qb5), Quaternary basaltic and andesitic rocks (Qb5a), Basaltic andesite of Aschoff Buttes (Qbaa), Quaternary volcanics, cinder cones (Qcc), Intrusive basalt and basaltic andesite (Qiba), Rocks of Sandy Glacier volcano (Qsg), Basalt and basaltic andesite (QTb), Boring Lava (QTb), Boring Lavas (QTb), Older basalt and basaltic andesite (QTb), Quaternary-Tertiary intrusions (QTi), Mafic vent complexes (QTmv), Andesite (QTtla2), Basalt (QTtlb), Volcanic rocks of the High Cascade Range and Boring Lava (QTv), Volcanic rocks, undifferentiated (QTv), Undifferentiated Boring Lava (Qtvu), Cinder cone or small volcano (Qv), Basaltic andesite and basalt flows, unnamed (Qvba), Andesite (Ta), Tertiary andesitic rocks (Ta2), Tertiary andesitic rocks (Ta2a), Andesite of Lolo Pass (Taop), Andesite of Salmon Butte (Tas), Andesite of Zigzag Mountain (Tazm), Ridge-capping basalt and basaltic andesite (Tb), Breitenbush Formation (Tb), Tertiary basaltic and basaltic andesitic rocks (Tb1), Andesitic and basaltic rocks (Tba), Basaltic andesite of Mack Hall Creek (Tbam), Basaltic andesite of the Oak Grove Fork (Tbao), Basalt of Bull Run Watershed and other ridge capping basalt (Tbbu), basalt of Canemah (Tbc), Basaltic andesite and basalt of Collawash Mountain (Tbc), Beds of Bull Creek (Tbc), basaltic andesite of Fallsview (Tbf), Basalt near Ghost Creek (Tbg), Tillamook Volcanics, upper plagioclase porphyritic basalt (Tbpu), Tillamook Volcanics, upper submarine basalt lapilli tuff and breccia (Tbru), Tillamook Volcanics, Upper porphyritic basalt flows (Tbu), Dacite of Plaza Lake (Tdp), Elk Lake Formation (Te), Fine-grained andesite (Tfa), Flows and clastic rocks, undivided (Tfc), Sentinel Bluffs member (Tgsb), Hornblende-bearing andesite (Tha), Basalt of Hembre Ridge (Thpb), Basalt intrusives (Ti), Intrusive rocks, undifferentiated (Ti), Mafic intrusions (Ti), Tertiary Intrusive rocks (Ti), Undifferentiated Tertiary intrusions (Ti), Undifferentiated Tertiary intrusions (Ti1), Intrusive andesite (Tia1), porphyritic basalt (Tiab), Basalt (Tib), Intrusive basalt and basaltic andesite (Tiba), Diabase (Tidb), Pyroxene-Hornblende Dacite of South Dickey Peak (Tidc), Hornblende Andesite Porphyry of Bull-of-the-Woods (Tiha), Hornblende Andesite/Diorite (Tiha), Hornblende Diorite of Elk Lake Creek (Tihd), Intrusive rocks of Laurel Hill (Tilh), Pyroxene Andesite Porphyry of Big Slide Mountain (Tipa), Pyroxene Andesite/Diorite (Tipa), Pyroxene Andesite/Diorite (Tipa1), Quartz Andesite (Tiqa), Hornblende Quartz Diorite Porphyry of Twin Lakes (Tiqd), Vitrophyre of Trout Creek (Titc), Little Butte volcanic rocks-older basalts (Tlb), Little Butte Volcanic Series (Tlb), Little Butte Volcanics (Tlb), Little Butte Volcanics, porphyritic andesite (Tlba), Little Butte Volcanics, basalt and basaltic andesite (Tlbb), Sardine Formation, lower member (Tlm), Molalla Formation (Tm), Andesite of middle and late Miocene age (Tma), Molalla Formation (Tmo), Andesite of Nohorn Creek (Tn), Outerson Formation (To), Older andesite (Toa), Quaternary volcanics, flows of basaltic andesite and basalt, pyroclastic tuff, and breccia (Tpv), Rocks of Barlow Ridge and Gunsight Butte (Trbg), Sardine Formation (Ts), Sardine Formation (Tsa), Sardine Formation, Tuff of Pansy Basin (Tsa1), Sardine Formation, Hornblende Ignimbrite of North Dickey Peak (Tsa2), Sardine Formation, Andesite Lava of Schreine Peak (Tsa3), Sardine Formation, andesite (Tsaa), Sardine Formation, volcanic rocks, undivided (Tsau), Sardine Formation, volcanic rocks (Tsav), Scorpion Mountain lavas (Tsm), Skamania Volcanic Series (Tsv), Andesite (Ttla1), Basalt and basaltic andesite flows and flow breccias (Tub), Sardine Formation, upper member (Tum), Cinder cone or small volcano (Tv), Cinder cone or small volcano (Tv1), Canemah tephra (Tvc), Fallsview tephra (Tvf), Goble Volcanics Tuff (Tgvt), Goble Volcanics Basaltic Andesite (Tgvb), Basalt-Cobble Conglomerate (Tbc), Wanapum Basalt (Twfs), Grande Ronde Basalt Member: Sentinel Bluffs (Tgsb), Frenchman Springs Basalt (Twf), Goble Volcanics (Tgo1), Basaltic Andesite Flow (Tgo2), Tillamook Volcanics (Ttv), Late Eocene Cole Mountain Basalt (Tcm), Goble Volcanics (Tg),	C
Water	Snow and ice (glacier)	C
Water	Water (water)	E

Table B-4. Soil amplification classification for geologic units from Burns and others (2011), Mickelson and Burns (2012), Burns and others (2015), Burns (2017), and this study. NEHRP is National Earthquake Hazard Reduction Program.

General Description	Map Unit Name and Abbreviation	NEHRP Class
Alluvium	Higher Sandy River terrace (Qts)	D
Alluvium	Alluvium (Qal), Alluvium (Qal1), Alluvium of the Sandy River (Has), Recent Alluvium (Qa1)	E
Colluvium	Glacial deposits (Qgd)	C
Colluvium	Fan (Qf), Pyroclastic flow (Qhpc)	D
Colluvium	Landslide (Qls), Landslide, Fan, Talus (Qls)	F
Sedimentary Bedrock	Residual Soil on Sedimentary Rock	C
Volcanic Bedrock	Intact Igneous Rock, Residual Soil on Igneous Rock	C

Table B-5. Hazus liquefaction classification for geologic units from Ma and others (2012).

General Description	Map Unit Name and Abbreviation	Hazus Class
Aeolian Deposits	Floodplain dune deposits (Hfd)	3
Aeolian Deposits	Eolian deposits (Qe), Primary loess (Ql)	4
Alluvium	Clackamas River terraces undifferentiated (Qtcx), Estacada terrace of the Clackamas River (Htce), Middle Clackamas terraces (Qtcm), Subterraces of the Estacada Terrace of the Clackamas River (Htcx), Subterraces of the middle terrace of the Clackamas River (Qtcmx), Upper Clackamas River terrace (Qtcu)	3
Alluvium	Pond Deposits (Qp), Terrace deposits of the Sandy River (Qtsu), Terrace deposits of the Tualatin Mountains (Qttm), Terrace deposits of the Willamette River (Htw), Terraces of Abernathy Creek (Hta)	4
Alluvium	Alluvium of lowland streams (Hal), Alluvium of minor streams (Qal), Alluvium of the Clackamas River (Hacl), Alluvium of the Columbia River (Haco), Alluvium of the Molalla-Pudding Rivers (Ham), Alluvium of the Sandy River (Has), Alluvium of the Tualatin River (Hat), Alluvium of the Willamette River (Haw), Sandy River volcanogenic delta (Hsd)	5
Artificial Fill	Artificial fill (Aaf)	5
Missoula Flood Deposits	Missoula flood deposits, coarse-grained facies (Qmc)	2
Missoula Flood Deposits	Missoula flood deposits, channel facies (Qmch), Missoula flood deposits, fine-grained (Qmf), Missoula floods silt colluvium (Qmf-c)	3
Sedimentary Bedrock	Hillsboro Formation (QTh), Rhododendron Formation (Tr), Scappoose Formation (Ts), Springwater Formation (QTs), Troutdale Formation, conglomerate (Ttg), Troutdale Formation, mudstone facies (Ttm), Troutdale Formation, sandstone (Tts)	0
Sedimentary Bedrock with Loess	Hillsboro Formation and loess (QTh-l), Springwater Formation and loess (QTs-l), Troutdale Formation, conglomerate (Ttg-l)	3
Volcanic Bedrock	Basalt of Borges Road (Qbr), Basalt of Canemah (Tbc), Basalt of Carver (Qbca), Basalt of Cooks Butte (Tbcb), Basalt of Douglass Ridge (Qbd), Basalt of Gingko (Twfg), Basalt of Jenne (Qbj), Basalt of Kelly Butte (Qbkb), Basalt of Mount Scott (Qbs), Basalt of Mount Sylvania (Qbsy), Basalt of Mount Tabor (Qbmt), Basalt of Mount Talbert (Qbm), Basalt of Powell Butte (Qbp), Basalt of Sand Hollow (Twfsh), Basalt of Sentinel Gap (Twfsg), Basalt of Tong Road (QTbt), Basalt of Umtanum (Tgu), Basalt of Waverly Heights and associated undifferentiated sedimentary rocks (Twh), Basalt of Winston Road (Qbw), Basalt of Zion Hill (QTbz), Basaltic andesite of Anderson (Qba), Basaltic andesite of Barnes Road (Qbab), Basaltic andesite of Beaver Creek (Tbb), Basaltic andesite of Broughton Bluff (Qbbb), Basaltic andesite of Fallsview (Tbf), Basaltic andesite of Hardscrabble (Qbhs), Basaltic andesite of Highland Butte (Tbh), Basaltic andesite of Hunsinger (Qbh), Basaltic andesite of Outlook (Qbo), Basaltic andesite of Rocky Butte (Qbrb), Basaltic andesite of Root Creek (Tbr), Canemah tephra (Tvc), Fallsview tephra (Tvf), Ortley Member (Tgo), Outlook tephra (Qvo), Root Creek tephra (Tvr), Sentinel Bluffs Member (Tgsb), Tephra of basalt of Rodlun Road (Qvrr), Undifferentiated Columbia River Basalt Group (Tcr), Undifferentiated Grande Ronde Basalt (Tgr), Undivided basalt and basaltic andesite (QTb), Volcanic sandstone and conglomerate (Qvca), Winter Water Member (Tgww), N2 and R2 Flows Undivided (Tgru)	0
Volcanic Bedrock with Loess	Basalt of Gingko (Twfg-l), Basalt of Kaiser Road and loess (Qbk-l), Basalt of Mount Sylvania and loess (Qbsy-l), Basalt of Rodlun Road and loess (Qbrr-l), Basalt of Sand Hollow (Twfsh-l), Basalt of Wapshilla Ridge and loess (Tgwr-l), Basalt of Waverly Heights and loess (Twh-l), Basaltic andesite of Bonny Slope and loess (QTbb-l), Basaltic andesite of Elk Point and loess (Qbae-l), Ortley Member (Tgo-l), Sentinel Bluffs Member and loess (Tgsb-l), Tephra of Jenne and loess (Qvj-l), Undifferentiated Columbia River Basalt Group (Tcr-l), Winter Water Member and loess (Tgww-l)	3

Table B-6. Hazus liquefaction classification for geologic units from R. Wells and others (unpub. data, 2017).

General Description	Map Unit Name and Abbreviation	Hazus Class
Aeolian Deposits	Floodplain dune deposits (Hfd)	3
Aeolian Deposits	Eolian deposits (Qe), Primary loess (Ql)	4
Alluvium	Clackamas River terraces undifferentiated (Qtcx), Estacada terrace of the Clackamas River (Htce), Middle Clackamas terraces (Qtcm), Subterraces of the Estacada Terrace of the Clackamas River (Htcx), Subterraces of the middle terrace of the Clackamas River (Qtcmx), Upper Clackamas River terrace (Qtcu), Terrace Deposits (Qtd), Older terrace deposits (Qto), Older Gravel of Columbia River Origin (QTcr), Deposits of Ape Canyon and Older (Qsa)	3
Alluvium	Alluvium of lowland streams (Hal), Alluvium of minor streams (Qal), Alluvium of the Clackamas River (Hacl), Alluvium of the Columbia River (Haco), Alluvium of the Molalla-Pudding Rivers (Ham), Alluvium of the Sandy River (Has), Alluvium of the Tualatin River (Hat), Alluvium of the Willamette River (Haw), Sandy River volcanogenic delta (Hsd), Alluvium (Qa)	5
Alluvium	Lacustrine Deposits (Qla)	4
Artificial Fill	Artificial fill (Aaf), Artificial Fill (af)	5
Colluvium	Basaltic colluvium (Qcb), Talus (Qt)	2
Missoula Flood Deposits	Missoula flood deposits, coarse-grained facies (Qmc), Coarse Grained Missoula Flood Deposits (Qfc)	2
Missoula Flood Deposits	Missoula flood deposits, channel facies (Qmch), Missoula flood deposits, fine-grained (Qmf), Missoula floods silt colluvium (Qmf-c), Missoula Flood Deposits (Qf)	3
Sedimentary Bedrock	Hillsboro Formation (QTh), Rhododendron Formation (Tr), Scappoose Formation (Ts), Springwater Formation (QTs), Troutdale Formation, conglomerate (Ttg), Troutdale Formation, mudstone facies (Ttm), Troutdale Formation, sandstone (Tts), Scappoose Formation: Dairy Creek Member (Tsdc), Mist Formation: Gus Creek conglomerate (Tmgc), Cowlitz Formation: Upper mudstone member (Tc2), Keasey Formation: Middle member (Tkm), Keasey Formation, Upper member (Tku), Hamlet Formation: Sweet Home Creek Member (Thsw), Pittsburg Bluff Formation: East Fork Member (Tpe), Pittsburg Bluff Formation: Pebble Creek Member (Tpp), Keasey Formation: Jewell member (Tkj), Scappoose Formation: Divide Member (Tsd), Cowlitz Formation: C&W sandstone member (Tc1), Mist Formation: Windy Ridge member (Tmwr), Hamlet Formation: Roy Creek Member (Thr), Hamlet Formation: Sunset Highway Member (Ths), Keasey Formation (Tk), Pittsburg Bluff Formation (Tpb), Sager Creek Formation (Tsc)	0
Sedimentary Bedrock with Loess	Hillsboro Formation and loess (QTh-l), Springwater Formation and loess (QTs-l), Troutdale Formation, conglomerate (Ttg-l)	3
Volcanic Bedrock	Basalt of Borges Road (Qbr), Basalt of Canemah (Tbc), Basalt of Carver (Qbca), Basalt of Cooks Butte (Tbcb), Basalt of Douglass Ridge (Qbd), Basalt of Gingko (Twfg), Basalt of Jenne (Qbj), Basalt of Kelly Butte (Qbkb), Basalt of Mount Scott (Qbs), Basalt of Mount Sylvania (Qbsy), Basalt of Mount Tabor (Qbmt), Basalt of Mount Talbert (Qbm), Basalt of Powell Butte (Qbp), Basalt of Sand Hollow (Twfsh), Basalt of Sentinel Gap (Twfsg), Basalt of Tong Road (QTbt), Basalt of Umtanum (Tgu), Basalt of Waverly Heights and associated undifferentiated sedimentary rocks (Twh), Basalt of Winston Road (Qbw), Basalt of Zion Hill (QTbz), Basaltic andesite of Anderson (Qba), Basaltic andesite of Barnes Road (Qbab), Basaltic andesite of Beaver Creek (Tbb), Basaltic andesite of Broughton Bluff (Qbbb), Basaltic andesite of Fallsview (Tbf), Basaltic andesite of Hardscrabble (Qbhs), Basaltic andesite of Highland Butte (Tbh), Basaltic andesite of Hunsinger (Qbh), Basaltic andesite of Outlook (Qbo), Basaltic andesite of Rocky Butte (Qbrb), Basaltic andesite of Root Creek (Tbr), Canemah tephra (Tvc), Fallsview tephra (Tvf), Ortley Member (Tgo), Outlook tephra (Qvo), Root Creek tephra (Tvr), Sentinel Bluffs Member (Tgsb), Tephra of basalt of Rodlun Road (Qvrr), Undifferentiated Columbia River Basalt Group (Tcr), Undifferentiated Grande Ronde Basalt (Tgr), Undivided basalt and basaltic andesite (QTb), Volcanic sandstone and conglomerate (Qvca), Winter Water Member (Tgww), Grande Ronde Basalt: Intrusive (Tig), Grande Ronde Basalt: N2 and R2 flows (Tgru), Grande Ronde Basalt: Grouse Creek Member (Tggc), Goble Volcanics (Togv), Grande Ronde Basalt: Wapshilla Ridge Member (Tgwr), Intrusive Wanapum Basalt (Tiw), Scaponia Tuff (Tps), Older Intrusions of the Western Cascade Range (Tio), Clastic Rocks Associated with Grande Ronde Basalt (Tgc), Grouse Creek Member (Tgr2)	0
Volcanic Bedrock with Loess	Basalt of Gingko (Twfg-l), Basalt of Kaiser Road and loess (Qbk-l), Basalt of Mount Sylvania and loess (Qbsy-l), Basalt of Rodlun Road and loess (Qbrr-l), Basalt of Sand Hollow (Twfsh-l), Basalt of Wapshilla Ridge and loess (Tgwr-l), Basalt of Waverly Heights and loess (Twh-l), Basaltic andesite of Bonny Slope and loess (QTbb-l), Basaltic andesite of Elk Point and loess (Qbae-l), Ortley Member (Tgo-l), Sentinel Bluffs Member and loess (Tgsb-l), Tephra of Jenne and loess (Qvj-l), Undifferentiated Columbia River Basalt Group (Tcr-l), Winter Water Member and loess (Tgww-l)	3

Table B-7. Hazus liquefaction classification for geologic units from OGDC-6 (Smith and Roe, 2015).

General Description	Map Unit Name and Abbreviation	Hazus Class
Aeolian	Primary Loess (Ql)	4
Alluvium	Sand and gravel that predates Missoula Floods (Qg2)	2
Alluvium	High terrace gravels (Qt), Older alluvial deposits (Qoal), Older alluvial deposits (Qoal1), Outwash (Qo), Weathered terrace gravel (QTg)	3
Alluvium	Sand and gravel that postdates Missoula Floods (Qg1), Terrace gravels (Qtg)	4
Alluvium	Alluvial deposits (Qal), Alluvium (Qal), Alluvium of smaller streams (Qalf), Alluvium, undifferentiated (Qau), Floodplain deposits of the Willamette River and major tributaries (Qalc), Quaternary alluvium (Qal), Alluvium (Qa1), Terrace Deposits (Qt), Pond Deposits (Qp), Lacustrine Deposits (Qlc), Alluvium (Qal1), Alluvium (Qa)	5
Artificial Fill	Artificial fill (af)	5
Colluvium	Pre-CRB Conglomerate (Toc)	0
Colluvium	Glacial deposits (Qg), Glacial drift (Qt), Glacial moraine and outwash deposits (Qgl), Glacial till (Qg), Talus (Qt), Talus (Qta), Talus deposits (Qt), Till of Evans Creek age (Qget), Till of neoglacial age (Qgnt), Younger till (Qyt)	2
Colluvium	Pyroclastic flow and debris-flow deposits (Qhc), Pyroclastic flow and debris-flow deposits (Qhpc), Pyroclastic flow and debris-flow deposits (Qhtc), Pyroclastic-flow and debris-flow deposits (Qhoc)	3
Colluvium	Flow and Fan Deposits (Qf),	5
Missoula Flood Deposits	Coarse Missoula Flood deposits (Qfc), Cataclysmic Flood Deposits: Gravel Facies (Qfg)	2
Missoula Flood Deposit	Main body of fine-grained Missoula Flood deposits (Qff2), Missoula (Bretz) Flood deposits (Qff), Cataclysmic Flood Deposits: Silt and Sand Facies (Qfs), Missoula Flood Deposits (Qmf)	3
Mixed Bedrock	Tertiary and Quaternary volcanic and sedimentary rocks and deposits, undivided (Tv), Tuffaceous sedimentary rocks, basalt flows, and tuffs, undivided (Tu)	0
Mixed Colluvium and Alluvium	Fluvial and lacustrine(?) sedimentary deposits (Tfl)	0
Mixed Colluvium and Alluvium	Colluvial and alluvial slope deposits (Qca), Glacio-fluvial deposits (Qgf), Conglomerate (QTc)	2
Sedimentary Bedrock	Basaltic sandstone at Roy Creek (Tbs), Coal-bearing conglomerates and claystones (Tom3), Consolidated fluvial deposits (Tpf), Continental sedimentary rocks (Tcs), Fossiliferous sandstones and tuffaceous claystones (Tom1), Older sedimentary rocks (Tos), Quaternary sediment and sedimentary rocks, undivided (Qs), Rhododendron Formation (Tmpr), Rhododendron Formation (Tr), Rhododendron Formation (Trh), Sandstone of Trask River (Trsk), Sardine Formation, tuffaceous nonmarine sedimentary rocks (Tsat), Scotts Mills Formation (Tsm), Scotts Mills Formation, Abiqua Member (Tsma), Scotts Mills Formation, Crooked Finger Member (Tsmc), Scotts Mills Formation, undifferentiated (Tsm), Sedimentary rocks (Ts), Springwater Formation (QTs), Tertiary sedimentary rocks (Ts1), Tertiary sedimentary rocks (Ts3), Tertiary sedimentary rocks (Ts4), Troutdale Formation (QTt), Troutdale Formation (Tpt), Troutdale Formation (Tt), Troutdale Formation mudstone and siltstone (Ttm), Troutdale Formation volcaniclastic sandstone (Tts), Troutdale Formation, Lower Member (Ttl), Troutdale Formation, Upper Member (QTtu), Tuffaceous arkose (Tom2), Yamhill Formation (Ty), Yamhill Formation, lower tuff unit (Tyt), Younger sedimentary rocks (Tys), Scappoose Formation (Ts1), Pittsburg Bluff Formation: Connors Creek Member (Tpbcc), Pittsburg Bluff Formation (Tpb), Scappoose Formation: interbeds, shelf sandstone (Ts2), Keasey Formation (Tk), Sandy River Mudstone (Tsr), Troutdale Formation (Ttf), Astoria Formation (TA), Astoria Formation (TA1), Pittsburg Bluff Formation: Laminated Member (Tpl), Pittsburg Bluff Formation: Siltstone Member (Tps), Scappoose Formation: Shelf Sandstone Unit (Ts), Cowlitz Formation (Tc), Scappoose Formation: Shelf Sandstone (Tso), Troutdale Formation: Coarse Grained (QTtd), Cowlitz Formation: Clark and Wilson Sandstone Member (Tccw), Cowlitz Formation: Upper Mudstone Member (Tcum), Hamlet Formation: Sweet Home Creek Mudstone Member (Thsw), Undifferentiated Oligocene and Miocene Units (Tom), Hamlet Formation: Roy Creek Conglomerate Member (Thr), Hamlet Formation: Sunset Highway Sandstone Member (Thsh), Troutdale Formation (Ttd), Keasey Formation: Vesper Church Member (Tkv), Oligocene Sediment: Shelf Sandstone (Tos), Troutdale Formation (Tt)	0
Volcanic Bedrock	Andesite (QTtla2), Andesite (Ta), Andesite (Ttla1), Andesite and dacite lava (Qha), Andesite of Cabin Creek (Qac), Andesite of Enola Hill (Qae), Andesite of Hiyu Mountains (Qah), Andesite of Horseshoe Ridge (Qahr), Andesite of Lolo Pass (Taop), Andesite of middle and late Miocene age (Tma), Andesite of Nohorn Creek (Tn), Andesite of Salmon Butte (Tas), Andesite of Skyline Road (Qas), Andesite of Tom Dick and Harry Mountain (QTat), Andesite of Wapinitia Pass (Qaw), Andesite of Zigzag Mountain (Tazm), Andesite west of Clear Lake (Qacl), Andesitic and basaltic rocks (Tba), Basalt (QTb), Basalt (QTtlb), Basalt (Tib), Basalt and basaltic andesite (QTb), Basalt and basaltic andesite (QTba), Basalt and basaltic andesite flows and flow breccias (Tub), Basalt andesite (QTba), Basalt intrusives (Ti), Basalt near Ghost Creek (Tbg), Basalt of Bull Run Watershed and other ridge capping basalt (Tbbu), basalt of Canemah (Tbc), Basalt of Crutcher Bench (Qbc), Basalt of Hembre Ridge (Thpb), Basalt of Sand Hollow (Tfsh), Basalt of Silver Falls (Tfsf), Basaltic andesite and basalt (Qba), Basaltic andesite and basalt (QTba), Basaltic andesite and basalt flows, unnamed (Qvba), Basaltic andesite and basalt of Collawash Mountain (Tbc), Basaltic andesite of Aschoff Buttes (Qbaa), Basaltic andesite of Devil Canyon (Qbdc), basaltic andesite of Fallsview (Tbf), Basaltic andesite of Mack Hall Creek (Tbam), Basaltic andesite of Mirror Lake and Eureka Peak (QTbme), Basaltic andesite of Sisi Butte (Qbs), Basaltic andesite of the Oak Grove Fork (Tbao), Beds of Bull Creek (Tbc), Boring Lava (QTb), Boring Lavas (QTb), Breitenbush Formation (Tb), Canemah tephra (Tvc), Cinder cone or small volcano (Qv), Cinder cone or small volcano (Tv), Cinder cone or small volcano (Tv1), Columbia River Basalt Group (Tcr), Columbia River Basalt Group and related flows (Tc), Columbia River Basalt Group, Frenchman Springs Member (Tyfs), Columbia River Basalt Group, Grande Ronde Basalt, N1 Low MgO Chemical Type (Tgn1l), Columbia River Basalt Group, Grande Ronde Basalt, N2 Low MgO Chemical Type (Tgn2l), Columbia River Basalt Group, Grande Ronde Basalt, R2 Low MgO Chemical Type (Tgr2l), Columbia River Basalt Group, Grande Ronde Basalt, Winter Water Flow (Tgn2w), Columbia River Basalt group, lower part (Tcl), Columbia River Basalt Group, Pomona Member (Tp), Columbia River Basalt Group, Priest Rapids Member (Tpr), Columbia River Basalt Group, undivided (Tc), Columbia River Basalt Group, Wanapum Basalt, Frenchman Springs Member (Tf), Dacite of Frog Lake Buttes (Qdf), Dacite of Plaza Lake (Tdp), Diabase (Tidb), Dike (Dike), Dike (Dike1), Dikes (dike), Eagle Creek Formation (Tec), Elk Lake Formation (Te), Fallsview tephra (Tvf), Fault breccia (breccia), Fine-grained andesite (Tfa), Flows and clastic rocks, undivided (Tfc), Grande Ronde Basalt (Tgr), Grande Ronde Basalt, Middle Low MgO Geochemical Type (Tygr1), Grande Ronde Basalt, high Mg chemical type (Tgh), Grande Ronde Basalt, High MgO Geochemical Type (Tygr3), Grande Ronde Basalt, Lower Low MgO Geochemical Type (Tygr0), Grande Ronde Basalt, normal polarity unit 2 (Tcgn2), Grande Ronde Basalt, reversed polarity unit 2 (Tcgr2), Grande Ronde Basalt, undivided (Tgr), Grande Ronde Basalt, upper flows, normal magnetic polarity (Tgn2), Grande Ronde Basalt, Upper Low MgO Geochemical Type (Tygr2), High Cascade lavas, basalt and basaltic andesite (Qb), Hornblende Andesite Porphyry of Bull-of-the-Woods (Tiha), Hornblende Andesite/Diorite (Tiha), Hornblende Diorite of Elk Lake Creek (Tihd), Hornblende Quartz Diorite Porphyry of Twin Lakes (Tiqd), Hornblende-bearing andesite (Tha), Hornblende-bearing basaltic andesite (Qbh), Intrusive andesite (Tia1), Intrusive basalt (Tib), Intrusive basalt and basaltic andesite (Qiba), Intrusive basalt and basaltic andesite (Tiba), Intrusive rocks of Laurel Hill (Tilh), Intrusive rocks, undifferentiated (Ti), Lava (Qhol), Lava (Qhpl), Little Butte volcanic rocks-older basalts (Tlb), Little Butte Volcanic Series (Tlb), Little Butte Volcanics (Tlb), Little Butte Volcanics, basalt and basaltic andesite (Tlbb), Little Butte Volcanics, porphyritic andesite (Tlba), Mafic intrusions (Ti), Mafic vent complexes (QTmv), Molalla Formation (Tm), Molalla Formation (Tmo), N2 High MgO Chemical Type (Tgn2h), Older andesite (Toa), Older basalt and basaltic andesite (QTb), Older basaltic andesite (Qoba), Olivine basalt (Qob), Ortley and Umtanum members (Tgou), Outerson Formation (To), Porphyritic basalt (Tiab), Prineville Geochemical Type (Typv), Pyroxene Andesite Porphyry of Big Slide Mountain (Tipa), Pyroxene Andesite/Diorite (Tipa), Pyroxene Andesite/Diorite (Tipa1), Pyroxene-Hornblende Dacite of South Dickey Peak (Tidc), Quartz Andesite (Tiqa), Quaternary basaltic and andesitic rocks (Qb4), Quaternary basaltic and andesitic rocks (Qb5), Quaternary basaltic and andesitic rocks (Qb5a), Quaternary volcanics, cinder cones (Qcc), Quaternary volcanics, flows of basaltic andesite and basalt, pyroclastic tuff, and breccia (Tpv), Quaternary-Tertiary intrusions (QTi), Ridge-capping basalt and basaltic andesite (Tb), Rocks of Barlow Ridge and Gunsight Butte (Trbg), Rocks of Sandy Glacier volcano (Qsg), Sardine Formation (Ts), Sardine Formation (Tsa), Sardine Formation, andesite (Tsaa), Sardine Formation, Andesite Lava of Schreine Peak (Tsa3), Sardine Formation, Hornblende Ignimbrite of North Dickey Peak (Tsa2), Sardine Formation, lower member (Tlm), Sardine Formation, Tuff of Pansy Basin (Tsa1), Sardine Formation, upper member (Tum), Sardine Formation, volcanic rocks (Tsav), Sardine Formation, volcanic rocks, undivided (Tsau), Scorpion Mountain lavas (Tsm), Sentinel Bluffs member (Tgsb), Skamania Volcanic Series (Tsv), Tertiary andesitic rocks (Ta2), Tertiary andesitic rocks (Ta2a), Tertiary basaltic and basaltic andesitic rocks (Tb1), Tertiary Intrusive rocks (Ti), Tillamook Volcanics, upper plagioclase porphyritic basalt (Tbpu), Tillamook Volcanics, Upper porphyritic basalt flows (Tbu), Tillamook Volcanics, upper submarine basalt lapilli tuff and breccia (Tbru), Undifferentiated Boring Lava (Qtvu), Undifferentiated Tertiary intrusions (Ti), Undifferentiated Tertiary intrusions (Ti1), Vitrophyre of Trout Creek (Titc), Volcanic and volcaniclastic rocks of the western Cascade Range, undivided (Tvw), Volcanic rocks of the High Cascade Range and Boring Lava (QTv), Volcanic rocks, undifferentiated (QTv), Wanapum Basalt (Twp), Wanapum Basalt, Frenchman Springs member (Tcwf), Wanapum Basalt, Frenchman Springs Member (Twf), Wanapum Basalt, Priest Rapids member (Tcwpr), Wanapum Basalt, Priest Rapids Member (Twp), Winter Water member (Tgww), Yakima Basalt Subgroup of the Columbia River Basalt Group (Tyb), Yakima Basalt Subgroup Of The Columbia River Basalt Group (Tyb), Younger basalt and basaltic andesite (Qb), Younger basaltic andesite (Qyba), Grouse Creek Member (Tgr2), Grays River Volcanics (Tgrv), Wapshilla Ridge Member Basalt (Tgr1), Winter Water Member Basalt (Tgr3), Grande Ronde Basalt (Tgru), Grande Ronde Basalt Member: Winter Water (Tgww), Grande Ronde Basalts Member: Ortley (Tgo), Columbia River Basalt (Tcr), Grande Ronde Basalt: Low MgO (Tgl), Grande Ronde Basalt: High MgO (Tgh), Grande Ronde Basalt (Tgr), Grays River Volcanics Basalt (Tgv), Columbia River Basalt Group (Tco), Columbia River Basalt Group (Tcrb), Goble Volcanics Tuff (Tgvt), Goble Volcanics Basaltic Andesite (Tgvb), Basalt-Cobble Conglomerate (Tbc), Wanapum Basalt (Twfs), Grande Ronde Basalt Member: Sentinel Bluffs (Tgsb), Frenchman Springs Basalt (Twf), Goble Volcanics (Tgo1), Basaltic Andesite Flow (Tgo2), Tillamook Volcanics (Ttv), Late Eocene Cole Mountain Basalt (Tcm), Goble Volcanics (Tg)	0
Water	Snow and ice (glacier)	2
Water	Water (water)	5

Table B-8. Hazus liquefaction classification for geologic units from Burns and others (2011), Mickelson and Burns (2012), Burns and others (2015), Burns (2017), and this study.

General Description	Map Unit Name and Abbreviation	Hazus Class
Alluvium	Alluvium (Qal), Alluvium (Qal1), Alluvium of the Sandy River (Has), Recent Alluvium (Qa1)	5
Alluvium	Higher Sandy River terrace (Qts)	3
Colluvium	Glacial deposits (Qgd)	2
Colluvium	Fan (Qf), Pyroclastic flow (Qhpc)	3
Sedimentary Bedrock	Residual Soil on Sedimentary Rock	0
Volcanic Bedrock	Intact Igneous Rock, Residual Soil on Igneous Rock	0

Table B-9. Hazus landslide susceptibility classification for geologic units from Ma and others (2012).

General Description	Map Unit Name and Abbreviation	Landslide Susceptibility Class
Aeolian Deposits	Eolian deposits (Qe), Floodplain dune deposits (Hfd), Loess (Ql), Primary loess (Ql)	B
Alluvium	Alluvium of lowland streams (Hal), Alluvium of minor streams (Qal), Alluvium of the Clackamas River (Hacl), Alluvium of the Columbia River (Haco), Alluvium of the Molalla-Pudding Rivers (Ham), Alluvium of the Sandy River (Has), Alluvium of the Tualatin River (Hat), Alluvium of the Willamette River (Haw), Clackamas River terraces undifferentiated (Qtcx), Estacada terrace of the Clackamas River (Htce), Middle Clackamas terraces (Qtcm), Sandy River volcanogenic delta (Hsd), Subterraces of the Estacada Terrace of the Clackamas River (Htcx), Subterraces of the middle terrace of the Clackamas River (Qtcmx), Terrace deposits of the Sandy River (Qtsu), Terrace deposits of the Tualatin Mountains (Qttm), Terrace deposits of the Willamette River (Htw), Terrace Deposits of Tualatin Mountains (Qttm), Terraces of Abernathy Creek (Hta), Upper Clackamas River terrace (Qtcu)	B
Artificial Fill	Artificial fill (Aaf)	C
Colluvium	Landslide (Qls)	C
Missoula Flood Deposits	Missoula flood deposits, channel facies (Qmch), Missoula flood deposits, coarse-grained facies (Qmc), Missoula flood deposits, fine-grained (Qmf), Missoula floods silt colluvium (Qmf-c)	B
Sedimentary Bedrock	Hillsboro Formation (QTh), Rhododendron Formation (Tr), Scappoose Formation (Ts), Springwater Formation (QTs), Troutdale Formation (Tt), Troutdale Formation, conglomerate (Ttg), Troutdale Formation, mudstone facies (Ttm), Troutdale Formation, sandstone (Tts)	B
Sedimentary Bedrock with Loess	Hillsboro Formation and loess (QTh-l), Springwater Formation and loess (QTs-l), Troutdale Formation, conglomerate (Ttg-l)	B
Volcanic Bedrock	Basalt of Borges Road (Qbr), Basalt of Canemah (Tbc), Basalt of Carver (Qbca), Basalt of Cooks Butte (Tbcb), Basalt of Douglass Ridge (Qbd), Basalt of Gingko (Twfg), Basalt of Jenne (Qbj), Basalt of Kelly Butte (Qbkb), Basalt of Mount Scott (Qbs), Basalt of Mount Sylvania (Qbsy), Basalt of Mount Tabor (Qbmt), Basalt of Mount Talbert (Qbm), Basalt of Powell Butte (Qbp), Basalt of Sand Hollow (Twfsh), Basalt of Sentinel Gap (Twfsg), Basalt of Tong Road (QTbt), Basalt of Umtanum (Tgu), Basalt of Waverly Heights and associated undifferentiated sedimentary rocks (Twh), Basalt of Winston Road (Qbw), Basalt of Zion Hill (QTbz), Basaltic andesite of Anderson (Qba), Basaltic andesite of Barnes Road (Qbab), Basaltic andesite of Beaver Creek (Tbb), Basaltic andesite of Broughton Bluff (Qbbb), Basaltic andesite of Fallsview (Tbf), Basaltic andesite of Hardscrabble (Qbhs), Basaltic andesite of Highland Butte (Tbh), Basaltic andesite of Hunsinger (Qbh), Basaltic andesite of Outlook (Qbo), Basaltic andesite of Rocky Butte (Qbrb), basaltic andesite of Root Creek (Tbr), Canemah tephra (Tvc), Fallsview tephra (Tvf), N2 and R2 flows (Tgru), Ortley Member (Tgo), Outlook tephra (Qvo), Root Creek tephra (Tvr), Sentinel Bluffs Member (Tgsb), Tephra of basalt of Rodlun Road (Qvrr), Undifferentiated Columbia River Basalt Group (Tcr), Undifferentiated Grande Ronde Basalt (Tgr), Undivided basalt and basaltic andesite (QTb), Volcanic sandstone and conglomerate (Qvca), Winter Water Member (Tgww)	A
Volcanic Bedrock with Loess	Basalt of Gingko (Twfg-l), Basalt of Kaiser Road and loess (Qbk-l), Basalt of Mount Sylvania and loess (Qbsy-l), Basalt of Rodlun Road and loess (Qbrr-l), Basalt of Sand Hollow (Twfsh-l), Basalt of Wapshilla Ridge and loess (Tgwr-l), Basalt of Waverly Heights and loess (Twh-l), Basaltic andesite of Bonny Slope and loess (QTbb-l), Basaltic andesite of Elk Point and loess (Qbae-l), Ortley Member (Tgo-l), Ortley Member with Loess (Tgo-l), Sentinel Bluffs Member and loess (Tgsb-l), Tephra of Jenne and loess (Qvj-l), Undifferentiated Columbia River Basalt Group (Tcr-l), Winter Water Member and loess (Tgww-l)	B
Water	water	B

Table B-10. Hazus landslide susceptibility classification for geologic units from R. Wells and others (unpub. data, 2017).

General Description	Map Unit Name and Abbreviation	Landslide Susceptibility Class
Aeolian Deposits	Eolian deposits (Qe), Loess (Ql)	B
Alluvium	Alluvial fan deposits (Qaf), Alluvium (Qa), Alluvium (Qal), Gravel of Coast Range provenance (Qgcr), Lacustrine deposits (Qla), Older gravel of Cascade arc origin (QTca), Older Gravel of Columbia River origin (QTcr), Older terrace deposits (Qto), Oldest, pre-Missoula deposits (Qh1), Terrace deposits (Qtd), Younger terrace deposits (Qty), Youngest deposits (Qh3), Deposits of Ape Canyon (Qsa)	B
Artificial Fill	Artificial fill (af)	C
Colluvium	Basaltic colluvium (Qcb), Colluvium (Qcb), Fan (Qf), Landslide (Qls), Talus (Qt), Talus Deposits (Qt)	C
Missoula Flood Deposits	Coarse Grained Missoula Flood Deposits (Qfc), Missoula Flood deposits (Qf)	B
Sedimentary Bedrock	C&W sandstone member (Tc1), Cowlitz Formation (Tc), Cowlitz Formation (Tc1), Cowlitz Formation (Tc2), Dairy Creek Member (Tsdc), Divide Member (Tsd), East Fork Member (Tpe), Gus Creek conglomerate (Tmgc), Hamlet Formation (Th), Hyaloclastite sandstone (Tth), Jewell member (Tkj), Keasey Formation (Tk), Keasey Formation, Jewell Member (Tkj), Keasey Formation, Middle Member (Tkm), Keasey Formation, Upper Member (Tku), Middle (Tkm), Oak Ranch Creek Member (Tsoc), Pebble Creek Member (Tpp), Pittsburg Bluff Formation (Tpb), Ribbon Ridge member (Tsrs), Roy Creek Member (Thr), Sager Creek Formation (Tsc), Sandy River Mudstone (Tsm), Scappoose Formation (Ts), Scappoose Formation of Warren and others (1945, 1946) (Ts), Silty interbeds (Tsrf), Stimson Mill Member (Tpsm), Sunset Highway Member (Ths), Sweet Home Creek Member (Thsw), Troutdale Formation, Conglomerate Member (Ttc), Tuff bed (Tpst), Upper member (Tku), Upper mudstone member (Tc2), Windy Ridge member (Tmwr), Windy Ridge Member (Tmwr), Yamhill Formation (Ty), Vantage Member (Tv)	B
Volcanic Bedrock	1.4-1.7 Ma (QTb3), 2.2-2.7 Ma (QTb1), Andesite (Tyva), Armstrong Canyon member (Tgac), Basalt (Thb), Basalt of Gingko of Mackin (1961) (Twfg), Basalt of Rosalia of Beeson and others (1989) (Twpr), Basalt of Sand Hollow of Mackin (1961) (Twfh), Basalt of Sentinel Gap of Mackin (1961) (Twfs), Buttermilk Canyon member (Tgbc), Clastic rocks associated with Grande Ronde Basalt (Tgc), Downey Gulch Member (Tgdg), Frenchman Springs Member (Twf), Goble Volcanics (Togv), Grouse Creek Member (Tggc), Intrusive Grande Ronde Basalt (Tig), Intrusive Wanapum Basalt (Tiw), Invasive Grande Ronde Basalt (Tig), N2 and R2 flows (Tgru), N2 flows (TgN2), Ortley Member (Tgo), R2 Flows undivided, Basalt (TgR2), Scaponia Tuff (Tps), Sentinel Bluff Member (Tgsb), Subaerial flows (Ttva), Subaerial rocks (Tsra), Submarine flows and breccias (Tsrm), Submarine flows and breccias (Ttvm), Tillamook Volcanics (Ttv), Tillamook Volcanics, Subaerial flows (Ttva), Umtanum Member (Tgu), Wapshilla Ridge Member (Tgwr), Winter Water Member (Tgww)	A
Water	Water (water)	B

Table B-11. Hazus landslide susceptibility classification for geologic units from OGDC-6 (Smith and Roe, 2015).

General Description	Map Unit Name and Abbreviation	Landslide Susceptibility Class
Alluvium	Alluvial deposits (Qal), Alluvium (Qa), Alluvium (Qal), Alluvium (Qal1), Alluvium of smaller streams (Qalf), Alluvium, undifferentiated (Qau), Floodplain deposits of the Willamette River and major tributaries (Qalc), Glacial drift (Qt), High terrace gravels (Qt), Higher Sandy River terrace (Qts), Older alluvial deposits (Qoal), Older alluvial deposits (Qoal1), Older Alluvium (Qa2), Older Terrace (Qot), Outwash (Qo), Quaternary alluvium (Qal), Recent Alluvium (Qa1), Sand and gravel that postdates Missoula Floods (Qg1), Sand and gravel that predates Missoula Floods (Qg2), Terrace (Qt), Weathered terrace gravel (QTg)	B
Artificial Fill	Artificial fill (af)	C
Colluvium	Glacial deposits (Qg), Glacial moraine and outwash deposits (Qgl), Glacial till (Qg), Till of Evans Creek age (Qget), Till of neoglacial age (Qgnt), Younger till (Qyt)	B
Colluvium	Colluvium (Qca), Fan (Qf), Landslide (Qls), Pyroclastic flow and debris-flow deposits (Qhc), Pyroclastic flow and debris-flow deposits (Qhpc), Pyroclastic flow and debris-flow deposits (Qhtc), Pyroclastic-flow and debris-flow deposits (Qhoc), Talus (Qt), Talus (Qta), Talus deposits (Qt)	C
Missoula Flood Deposits	Coarse Missoula Flood deposits (Qfc), Main body of fine-grained Missoula Flood deposits (Qff2), Missoula (Bretz) Flood deposits (Qff)	B
Mixed Bedrock	Cinder cone or small volcano (Tv), Tuffaceous sedimentary rocks, basalt flows, and tuffs, undivided (Tu)	A
Mixed Bedrock	Colluvial and alluvial slope deposits (Qca), Fluvial and lacustrine(?) sedimentary deposits (Tfl), Tertiary and Quaternary volcanic and sedimentary rocks and deposits, undivided (Tv)	B
Mixed Colluvium and Alluvium	Glacio-fluvial deposits (Qgf)	B
Sedimentary Bedrock	Astoria Formation (TA), Astoria Formation (TA1), Basaltic sandstone at Roy Creek (Tbs), Coal-bearing conglomerates and claystones (Tom3), Consolidated fluvial deposits (Tpf), Continental sedimentary rocks (Tcs), Fossiliferous sandstones and tuffaceous claystones (Tom1), Keasey Formation (Tk), Older sedimentary rocks (Tos), Pittsburg Bluff Formation (Tpb), Pittsburg Bluff Formation, laminated member (TPl), Pittsburg Bluff Formation, siltstone member (TPs), Quaternary sediment and sedimentary rocks, undivided (Qs), Rhododendron Formation (Tmpr), Rhododendron Formation (Tr), Rhododendron Formation (Trh), Sandstone of Trask River (Trsk), Sardine Formation, tuffaceous nonmarine sedimentary rocks (Tsat), Scappoose Formation (Ts1), Scappoose Formation (Tso), Scappoose Formation, interbeds (Ts2), Scappoose Formation (Ts1), Scotts Mills Formation, Abiqua Member (Tsma), Scotts Mills Formation, Crooked Finger Member (Tsmc), Scotts Mills Formation, undifferentiated (Tsm), Sedimentary rocks (Ts), Tertiary sedimentary rocks (Ts1), Tertiary sedimentary rocks (Ts3), Tertiary sedimentary rocks (Ts4), Troutdale Formation (QTt), Troutdale Formation (QTtd), Troutdale Formation (Tpt), Troutdale Formation (Tt), Troutdale Formation (Ttd), Troutdale Formation mudstone and siltstone (Ttm), Troutdale Formation volcaniclastic sandstone (Tts), Troutdale Formation, Lower Member (Ttl), Troutdale Formation, Upper Member (QTtu), Tuffaceous arkose (Tom2), Yamhill Formation (Ty), Yamhill Formation, lower tuff unit (Tyt), Younger sedimentary rocks (Tys)	B
Volcanic Bedrock	Andesite (QTtla2), Andesite (Ta), Andesite (Ttla1), Andesite and dacite lava (Qha), Andesite of Cabin Creek (Qac), Andesite of Enola Hill (Qae), Andesite of Hiyu Mountains (Qah), Andesite of Horseshoe Ridge (Qahr), Andesite of Lolo Pass (Taop), Andesite of middle and late Miocene age (Tma), Andesite of Nohorn Creek (Tn), Andesite of Salmon Butte (Tas), Andesite of Skyline Road (Qas), Andesite of Tom Dick and Harry Mountain (QTat), Andesite of Wapinitia Pass (Qaw), Andesite of Zigzag Mountain (Tazm), Andesite west of Clear Lake (Qacl), Andesitic and basaltic rocks (Tba), Basalt (QTb), Basalt (QTtlb), Basalt (Tib), Basalt and basaltic andesite (QTb), Basalt and basaltic andesite (QTba), Basalt and basaltic andesite flows and flow breccias (Tub), Basalt andesite (QTba), Basalt intrusives (Ti), Basalt near Ghost Creek (Tbg), Basalt of Bull Run Watershed and other ridge capping basalt (Tbbu), basalt of Canemah (Tbc), Basalt of Crutcher Bench (Qbc), Basalt of Hembre Ridge (Thpb), Basalt of Sand Hollow (Tfsh), Basalt of Silver Falls (Tfsf), Basaltic andesite and basalt (Qba), Basaltic andesite and basalt (QTba), Basaltic andesite and basalt flows, unnamed (Qvba), Basaltic andesite and basalt of Collawash Mountain (Tbc), Basaltic Andesite flow (Tgo2), Basaltic andesite of Aschoff Buttes (Qbaa), Basaltic andesite of Devil Canyon (Qbdc), basaltic andesite of Fallsview (Tbf), Basaltic andesite of Mack Hall Creek (Tbam), Basaltic andesite of Mirror Lake and Eureka Peak (QTbme), Basaltic andesite of Sisi Butte (Qbs), Basaltic andesite of the Oak Grove Fork (Tbao), Beds of Bull Creek (Tbc), Boring Lava (QTb), Boring Lavas (QTb), Breitenbush Formation (Tb), Cinder cone or small volcano (Qv), Cinder cone or small volcano (Tv1), Columbia River Basalt Group (Tco), Columbia River Basalt Group (Tcr), Columbia River Basalt Group and related flows (Tc), Columbia River Basalt Group, Frenchman Springs Member (Tyfs), Columbia River Basalt Group, Grande Ronde Basalt, N1 Low MgO Chemical Type (Tgn1l), Columbia River Basalt Group, Grande Ronde Basalt, N2 Low MgO Chemical Type (Tgn2l), Columbia River Basalt Group, Grande Ronde Basalt, R2 Low MgO Chemical Type (Tgr2l), Columbia River Basalt Group, Grande Ronde Basalt, Winter Water Flow (Tgn2w), Columbia River Basalt group, lower part (Tcl), Columbia River Basalt Group, Pomona Member (Tp), Columbia River Basalt Group, Priest Rapids Member (Tpr), Columbia River Basalt Group, undivided (Tc), Columbia River Basalt Group, Wanapum Basalt (TWfs), Columbia River Basalt Group, Wanapum Basalt, Frenchman Springs Member (Tf), Dacite of Frog Lake Buttes (Qdf), Dacite of Plaza Lake (Tdp), Diabase (Tidb), Dike (Dike), Dike (Dike1), Dikes (dike), Eagle Creek Formation (Tec), Elk Lake Formation (Te), Fallsview tephra (Tvf), Fault breccia (breccia), Fine-grained andesite (Tfa), Flows and clastic rocks, undivided (Tfc), Grande Ronde Basalt (Tgr), Grande Ronde Basalt, Middle Low MgO Geochemical Type (Tygr1), Grande Ronde Basalt, high Mg chemical type (Tgh), Grande Ronde Basalt, High MgO Geochemical Type (Tygr3), Grande Ronde Basalt, Lower Low MgO Geochemical Type (Tygr0), Grande Ronde Basalt, normal polarity unit 2 (Tcgn2), Grande Ronde Basalt, reversed polarity unit 2 (Tcgr2), Grande Ronde Basalt, undivided (Tgr), Grande Ronde Basalt, upper flows, normal magnetic polarity (Tgn2), Grande Ronde Basalt, Upper Low MgO Geochemical Type (Tygr2), Grays River Volcanics (Tgv), Grouse Creek Member (Tgr2), High Cascade lavas, basalt and basaltic andesite (Qb), Hornblende Andesite Porphyry of Bull-of-the-Woods (Tiha), Hornblende Andesite/Diorite (Tiha), Hornblende Diorite of Elk Lake Creek (Tihd), Hornblende Quartz Diorite Porphyry of Twin Lakes (Tiqd), Hornblende-bearing andesite (Tha), Hornblende-bearing basaltic andesite (Qbh), Intrusive basalt (Tib), Intrusive basalt and basaltic andesite (Qiba), Intrusive basalt and basaltic andesite (Tiba), Intrusive rocks of Laurel Hill (Tilh), Intrusive rocks, undifferentiated (Ti), Lava (Qhol), Lava (Qhpl), Little Butte volcanic rocks-older basalts (Tlb), Little Butte Volcanic Series (Tlb), Little Butte Volcanics (Tlb), Little Butte Volcanics, basalt and basaltic andesite (Tlbb), Little Butte Volcanics, porphyritic andesite (Tlba), Mafic intrusions (Ti), Mafic vent complexes (QTmv), Molalla Formation (Tm), Molalla Formation (Tmo), N2 High MgO Chemical Type (Tgn2h), Older andesite (Toa), Older basalt and basaltic andesite (QTb), Older basaltic andesite (Qoba), Olivine basalt (Qob), Ortley and Umtanum members (Tgou), Outerson Formation (To), Porphyritic basalt (Tiab), Prineville Geochemical Type (Typv), Pyroxene Andesite Porphyry of Big Slide Mountain (Tipa), Pyroxene Andesite/Diorite (Tipa), Pyroxene Andesite/Diorite (Tipa1), Pyroxene-Hornblende Dacite of South Dickey Peak (Tidc), Quaternary basaltic and andesitic rocks (Qb4), Quaternary basaltic and andesitic rocks (Qb5), Quaternary basaltic and andesitic rocks (Qb5a), Quaternary volcanics, cinder cones (Qcc), Quaternary volcanics, flows of basaltic andesite and basalt, pyroclastic tuff, and breccia (Tpv), Quaternary-Tertiary intrusions (QTi), Ridge-capping basalt and basaltic andesite (Tb), Rocks of Barlow Ridge and Gunsight Butte (Trbg), Rocks of Sandy Glacier volcano (Qsg), Sardine Formation (Ts), Sardine Formation (Tsa), Sardine Formation, andesite (Tsaa), Sardine Formation, Andesite Lava of Schreine Peak (Tsa3), Sardine Formation, Hornblende Ignimbrite of North Dickey Peak (Tsa2), Sardine Formation, lower member (Tlm), Sardine Formation, Tuff of Pansy Basin (Tsa1), Sardine Formation, upper member (Tum), Sardine Formation, volcanic rocks (Tsav), Sardine Formation, volcanic rocks, undivided (Tsau), Scorpion Mountain lavas (Tsm), Sentinel Bluffs member (Tgsb), Skamania Volcanic Series (Tsv), Tertiary andesitic rocks (Ta2), Tertiary andesitic rocks (Ta2a), Tertiary basaltic and basaltic andesitic rocks (Tb1), Tertiary Intrusive rocks (Ti), Tillamook Volcanics, upper plagioclase porphyritic basalt (Tbpu), Tillamook Volcanics, Upper porphyritic basalt flows (Tbu), Tillamook Volcanics, upper submarine basalt lapilli tuff and breccia (Tbru), Undifferentiated Boring Lava (Qtvu), Undifferentiated Tertiary intrusions (Ti), Undifferentiated Tertiary intrusions (Ti1), Vitrophyre of Trout Creek (Titc), Volcanic and volcaniclastic rocks of the western Cascade Range, undivided (Tvw), Volcanic rocks of the High Cascade Range and Boring Lava (QTv), Volcanic rocks, undifferentiated (QTv), Volcaniclastic sedimentary and volcanic rocks, Goble Volcanics (Tgo1), Wanapum Basalt (Twf), Wanapum Basalt (Twp), Wanapum Basalt, Frenchman Springs member (Tcwf), Wanapum Basalt, Frenchman Springs Member (Twf), Wanapum Basalt, Priest Rapids member (Tcwpr), Wanapum Basalt, Priest Rapids Member (Twp), Wapshilla Ridge Member (Tgr1), Winter Water Member (Tgr3), Winter Water member (Tgww), Yakima Basalt Subgroup of the Columbia River Basalt Group (Tyb), Yakima Basalt Subgroup Of The Columbia River Basalt Group (Tyb), Younger basalt and basaltic andesite (Qb), Younger basaltic andesite (Qyba)	A
Water	Snow and ice (glacier)	A
Water	Water (water)	B

Table B-12. Hazus landslide susceptibility classification for geologic units from Burns and others (2011), Mickelson and Burns (2012), Burns and others (2015), Burns (2017), and this study.

General Description	Map Unit Name and Abbreviation	Landslide Susceptibility Class
Alluvium	Alluvium (Qal), Alluvium (Qal1), Alluvium of the Sandy River (Has), Higher Sandy River terrace (Qts), Recent Alluvium (Qa1)	B
Colluvium	Glacial deposits (Qgd)	B
Colluvium	Fan (Qf), Landslide (Qls), Landslide (Qls), Landslide, Fan, Talus (Qls), Pyroclastic flow (Qhpc)	C
Sedimentary Bedrock	Residual Soil on Sedimentary Rock	B
Volcanic Bedrock	Intact Igneous Rock, Residual Soil on Igneous Rock	A

Table B-13. Lidar imagery used in this study.

Project Name	Acquisition Year	Organization	Rank by Most Recent Collection	Link
NW Oregon ODF - McGregor	2015	ODF	1	
NW Oregon ODF - Wilkerson	2015	ODF	2	
NW Oregon ODF - Salmonberry	2015	ODF	3	
NW Oregon ODF - Abiqua	2015	ODF	4	
NW Oregon ODF - Clatsop	2015	ODF	5	
Wasco 2015	2014 - 2015	OLC	6	https://www.oregongeology.org/pubs/ldq/reports/OLC_WASCO_County_Delivery_1_2_3_4_5_6_Data_Report.pdf
Metro 2014	2014	OLC	7	https://www.oregongeology.org/pubs/ldq/reports/OLC_Metro_2014_Data_Report-and_Hydroflattening_Project.pdf
Scappoose 2013	2013	OLC	8	https://www.oregongeology.org/pubs/ldq/reports/OLC_Scapoose_2013_Data_Report.pdf
Clackamol 2013	2013	OLC	9	https://www.oregongeology.org/pubs/ldq/reports/OLC_Clackamol_Data_Report_2013.pdf
Tillamook-Yamhill 2012	2012	OLC	10	https://www.oregongeology.org/pubs/ldq/reports/OLC_Tillamook-Yamhill_Final_Report_2012.pdf
Sandy River Bathymetric Survey 2012	2012	OLC	11	https://www.oregongeology.org/pubs/ldq/reports/Sandy_River_LiDAR_finalcompressed.pdf
Upper Sandy River	2011	OLC	12	https://www.oregongeology.org/pubs/ldq/reports/OLC_Upper_SANDY.pdf
Columbia River_USACE	2010	USACE	13	https://www.oregongeology.org/pubs/ldq/reports/Columbia_River_2010_Survey_Report.pdf
North Coast - Delivery 6	2009	OLC	14	https://www.oregongeology.org/pubs/ldq/reports/North_Coast_Lidar_Report_2009.pdf
North Coast - Delivery 7	2009	OLC	15	https://www.oregongeology.org/pubs/ldq/reports/North_Coast_Lidar_Report_2009.pdf
North Coast - Delivery 8	2009	OLC	16	https://www.oregongeology.org/pubs/ldq/reports/North_Coast_Lidar_Report_2009.pdf
North Coast - Delivery 5	2009	OLC	17	https://www.oregongeology.org/pubs/ldq/reports/North_Coast_Lidar_Report_2009.pdf
Willamette Valley 2009	2008 - 2009	OLC	18	https://www.oregongeology.org/pubs/ldq/reports/Willamette_Valley_Lidar_Report_2009.pdf
Sandy River	2008	USDA_FS	19	https://www.oregongeology.org/pubs/ldq/reports/Sandy_River_Lidar_Report_2008.pdf
Lower Salmon River	2007	Oregon Trout	20	https://www.oregongeology.org/pubs/ldq/reports/Lower_Salmon_River_2007_Surevy_Report.pdf
Hood to Coast 2009	2007	OLC	21	https://www.oregongeology.org/pubs/ldq/reports/PDX-Hood_Lidar_Report_2007.pdf
Lower Columbia 2005	2005	PSLC	23	https://www.oregongeology.org/pubs/ldq/reports/Lower_Columbia_River_2005_Survey_Report.pdf
Portland Pilot	2004	PSLC	22	

ODF is Oregon Department of Forestry. USACE is U.S. Army Corps of Engineers. OLC is Oregon Lidar Consortium. USDA_FS is U.S. Department of Agriculture (USDA) Forest Service. PSLC is Puget Sound Lidar Consortium.